A&A 396, 513–532 (2002)
DOI: 10.1051/0004-6361:20021362

Astronomy & Astrophysics

Stellar rotation and variability in the Orion Nebula Cluster[⋆,⋆⋆]

W. Herbst[1,2], C. A. L. Bailer-Jones[2], R. Mundt[2], K. Meisenheimer[2], and R. Wackermann[2]

[1] Van Vleck Obs., Wesleyan U., Middletown, CT 06459 USA
[2] Max-Planck-Institüt für Astronomie, Königstuhl 17, 69117 Heidelberg, Germany
e-mail: calj@mpia-hd.mpg.de, mundt@mpia-hd.mpg.de, meisenheimer@mpia-hd.mpg.de

Received 15 May 2002 / Accepted 18 September 2002

Abstract. A wide field imager attached to the MPG/ESO 2.2 m telescope on La Silla has been used to monitor the Orion Nebula Cluster on 45 nights between 25 Dec. 1998 and 28 Feb. 1999. Ninety-two images were obtained during this period through an intermediate band filter centered at 815.9 nm. More than 1500 sources with I magnitudes between 12.5 and 20 were monitored. We find that essentially every star brighter than 16th mag (where the precision is <0.01 mag) is a variable, with about half having a peak-to-peak variation of ~0.2 mag or more. A clear correlation is found between the level of variability and infrared excess emission, in the sense that stars with evidence for circumstellar disks have larger amplitudes of variation. A search for periodic variables was carried out and 369 such stars were discovered, most or all of which are rotating, spotted T Tauri stars. Periodic variables are most commonly found among the low amplitude variables. 46% of the stars with magnitudes between 12.5 and 16 and standard deviation, $\sigma < 0.1$ mag, were found to be periodic, whereas only 24% of the stars in the same magnitude range with $\sigma > 0.1$ yielded periods.
Our work confirms the existence of a bimodal period distribution, with peaks near 2 and 8 days, for stars with $M > 0.25\ M_{\odot}$ and a unimodal distribution peaked near 2 days, for lower mass stars. We show that a statistically significant correlation exists between infrared excess emission and rotation in the sense that slower rotators are more likely to show evidence of circumstellar disks. Slowly rotating stars, with angular velocities, $\omega < 1$ radian/d, corresponding to rotation periods longer than 6.28 d, have a mean infrared excess emission, $\Delta(I-K) = 0.55 \pm 0.05$, indicative of the presence of inner disks, while rapid rotators, with $\omega > 2$ radians/d, corresponding to rotation periods shorter than 3.14 d, have a much smaller mean of 0.17 ± 0.05. This supports the hypothesis that disks are involved in regulating stellar rotation during the pre-main sequence phase.
We explore a simple and commonly adopted model of rotational evolution in which stars conserve angular velocity while locked to a disk and conserve angular momentum once released. If these assumptions are valid, and if the locking period is 8 days, we find that more than half of the stars in the ONC are no longer locked to disks and that an exponential decay model with a disk-locking half-life of about 0.5–1 My fits the observations well. Assuming that the mean ages of the higher and lower mass stars are the same, the faster rotation of the lower mass stars can be understood as either a consequence of a shorter disk-locking time or a shorter initial disk-locking period, or both.

Key words. open clusters and associations: individual: Orion Nebula Cluster – stars: pre-main sequence – stars: rotation

1. Introduction

The Orion Nebula Cluster (ONC) is an excellent target for star formation studies since it contains thousands of pre-main sequence (PMS) stars within ~15′ (2 pc) of the central Trapezium stars (Herbig & Terndrup 1986; Hillenbrand & Hartmann 1998). The age of the cluster is ~1 My and it has a range of masses from ~25 $M_{\odot}$ (for θ^1 Ori C) down to below the hydrogen burning limit, and perhaps even below the deuterium burning limit (Hillenbrand 1997; Lucas & Roche 2000). At a distance of ~450 pc, its PMS stars are still relatively bright and not heavily embedded since much of the dust within the cluster has been cleared by radiation pressure and winds from the massive stars. A recent review of the Orion Nebula star forming region and its components has been provided by O'Dell (2001). The cluster is situated near the front face of a very dense cloud, so that nearly all of the stars within 15′ of the cluster center are cluster members (Jones & Walker 1988; Hillenbrand & Hartmann 1998).

The ONC is ideally suited for study with the Wide Field Imager (WFI) on the 2.2 m MPG/ESO telescope at the European Southern Observatory's (ESO) La Silla observing station in Chile. The field of view of this instrument just encompasses the cluster and the excellent seeing at La Silla

Send offprint requests to: W. Herbst,
e-mail: wherbst@wesleyan.edu

⋆ Figure 2 is only available in electronic form at http://www.edpsciences.org

⋆⋆ Full versions of Tables 1 to 3 are only available in electronic form at the CDS via anonymous ftp to cdsarc.u-strasbg.fr (130.79.128.5) or via http://cdsweb.u-strasbg.fr/cgi-bin/qcat?J/A+A/396/513

allows one to measure relatively faint stars even against the bright nebular background. Furthermore, the large number of photometric nights available during the southern hemisphere's summer months makes it an ideal location for a monitoring project. We, therefore, undertook a variability study of the ONC with this instrument during its commissioning phase from 1998 Dec. to 1999 Feb. and report the results here.

Almost every cluster member monitored is expected to be a variable star at some level, since they are all low mass, extremely young stars. In loose associations such stars are all either classical or weak-line T Tauri stars (CTTS and WTTS, respectively) and show optical variations ranging from a few hundredths of a magnitude to more than 3 mag. The variations are thought to be caused primarily by the rotational modulation of a spotted surface in the case of WTTS with the addition of a short time scale irregular component caused by accretion hot spots in the case of CTTS (e.g. Herbst et al. 1994). The spots on WTTS are cooler than their photospheres and presumably represent the footprints of strong magnetic fields that cover significant portions of the surfaces of these young, rapidly rotating and fully convective stars. Cool spots also exist on CTTS but probably in association with hot spots (or "zones") caused by magnetically-channeled accretion flows (e.g. Mahdavi & Kenyon 1998). It is also possible that stellar flares and/or occultation by circumstellar matter causes optical variations in some stars. In short, the ONC is a particularly propitious part of the sky in which to seek and study variable stars.

A number of variability studies have, of course, been carried out in this cluster, but only since the advent of CCDs are the data extensive and reliable. This is mostly because the background nebulosity is so bright and spatially variable and the low mass stars rather faint in the blue and visual parts of the optical spectrum, where photographic and photoelectric detectors are most sensitive. Optical CCD monitoring began with the Trapezium cluster – the inner few arc-minutes of the ONC – at the beginning of the last decade (Mandel & Herbst 1991) and the pace of the work accelerated as interesting results were obtained (Attridge & Herbst 1992; Eaton et al. 1995; Choi & Herbst 1996; Stassun et al. 1999; Herbst et al. 2000). Recently, an infrared variability study of the entire Orion A molecular cloud, including the ONC, was completed by Carpenter & Hillenbrand (2001). Also, it should be noted that Rebull (2001) has published a variability study of the so-called "flanking fields" on the perimeter, but not including, the ONC.

Most of the work to date has focused on the periodic variables, because it is easiest to extract useful information about the stars from their light curves. Approximately 200 periodic variables were known in the ONC prior to this study, from the investigations listed in the previous paragraph. Periodicity is caused by stellar rotation, so the accumulation and interpretation of these data is important for understanding stellar angular momentum evolution during the PMS phase. It has been known for more than a decade that CTTS are remarkably slow rotators (Bouvier et al. 1986; Hartmann et al. 1986), and must have shed large amounts of the angular momentum during the protostar or early PMS phase. Magnetic coupling to an accretion disk has been proposed as a dominant mechanism for accomplishing this (Camenzind 1990; Königl 1991; Shu et al. 1994). Observational support for that picture includes evidence for a correlation of rotation properties with the presence of disks (Bouvier et al. 1993; Edwards et al. 1993). However, that correlation and other evidence for disk-locking has recently been challenged by Stassun et al. (1999, hereinafter SMMV; cf. however, Herbst et al. 2000, hereinafter HRHC). In this paper, we will revisit the debate about disk-locking with a sample twice the size of that which has previously been employed.

Perhaps the most surprising result to arise from previous studies was the discovery by Attridge & Herbst (1992) of a bimodal period distribution for the brighter stars studied by them with a small (0.6m) telescope at Van Vleck Observatory (VVO). ONC stars were found to favor rotation periods near 2 and 8 days and avoid 4 days. This result was confirmed by Choi & Herbst (1996), but was part of the challenge raised by SMMV to the disk-locking hypothesis. They claimed that the period distribution in the ONC was not significantly different from uniform. The source of the conflcting interpretations has now been clarified by HRHC and by Herbst, Bailer-Jones & Mundt (2001; Paper I), the latter study based on the WFI data presented here. It turns out that rotation is mass-dependent in the ONC and that the brighter, more massive stars (with $M > 0.25\ M_{\odot}$) studied at VVO have, in fact, a bimodal period distribution, whereas the lower mass stars, more of which were included in the deeper survey of SMMV, have a unimodal distribution. These issues were already laid out in Paper I but will be revisited briefly here. The interpretation of disk-locking as the cause of the peak at 8 days in the rotational period distribution of the more massive stars remains the only viable hypothesis with a reasonable physical basis. The question of whether infrared data support this view or not is addressed here, as is the puzzle posed by the rapid rotation and apparently unimodal period distribution of the lower mass stars. A simple, stochastic model of disk evolution is also presented which can account for the rotation properties of all the stars in terms of the disk-locking hypothesis and allows us to derive a time scale for disk-locking. However, it is likely that more sophisticated models of angular momentum evolution will be required to fully account for the wealth of data now available.

2. Photometry

Observations were obtained on 45 nights during a two month interval from 25 Dec. 1998 to 22 Feb. 1999 with the WFI on the MPG/ESO 2.2 m telescope. Ninety-two images were obtained in total. Normally, 1–3 images were taken per night, with two of these usually coming one right after the other. All data were obtained through ESO filter 851, which is centered at 815.9 nm and has a full width at half maximum ($FWHM$) of 27 nm. It was chosen to minimize the nebular contamination while maximizing the signal from the faint, red stars which constitute the bulk of the cluster population. Its effective wavelength is close to that of the Cousins I system.

The WFI consists of 8 CCD's, each with 2048×4096 pixels, mounted in two rows so as to produce an approximately 8 K $\times$ 8 K array. Figure 1 shows the alignment of our fields with respect to the cluster. The extremely bright Trapezium stars (θ^1 Ori), which are located near the center of the ONC,

were deliberately placed in the central gap between CCD chips so that signal bleeding from what would have been their highly saturated images did not affect our frames. The width of the gaps between chips is 23.3″ (96 pixels) in right ascension and 14.3″ (60 pixels) in declination. The pixel scale is 0.238″/pixel and the size of the field is 33′ × 34′. About 4% of the surface area of the sky is lost due to the gaps, but variations in setting the telescope from night to night and edge effects on the CCDs effectively increase this to ∼10% for good photometric coverage. The average seeing at the 2.2 m for these observations was 0.9″ (*FWHM*) and the range was from 0.6″ to 1.8″.

All image processing was done using standard tasks in IRAF (Image Reduction and Analysis Facility distributed by the U. S. National Optical Astronomy Observatory). During the reductions, the 8 CCD chips were treated separately for all purposes, including flat fielding, differential photometry, and astrometry, as a matter of convenience. Flat fielding was accomplished using twilight flats taken each night or two. Average flats over about a week were employed in the reductions since there was no evidence of significant changes on this timescale. The images were aligned using IMALIGN to a common reference frame chosen because of its excellent seeing and accurate positioning at the nominal central location. The reference image is available electronically as Fig. 2.

A source list was formed by employing DAOFIND on the reference image with the search set for round objects of sufficient sharpness that were 5σ above the sky noise. This resulted in detection of all the stars of interest (i.e. those bright enough to be monitored photometrically) plus some things (image artifacts, in particular) that were not interesting. A visual inspection of the image was used to weed out as many of the non-stellar sources as possible. In some regions near the center of the cluster it was necessary to remove many sources that were not stars but merely bright spots in the nebula. It should be noted that the final source list is not uniform across the field in terms of its limiting magnitude, because of the nebulosity. Our principal goal was to include every *bona fide* star which was of sufficient brightness ($I \sim 18$ mag) to yield a precision of ∼0.05 mag or better in our source list. A visual inspection of the images suggests that we have succeeded in this regard except, perhaps, in the very inner parts of the cluster, where nebular contamination is severe. Altogether we performed photometry on 2294 objects, but those fainter than 20th mag or too close to the edges of the frames did not yield sufficiently precise results to warrant inclusion in the published source list. The 1562 remaining stars are listed in Table 1.

The IRAF tasks CCXYMATCH and CCMAP were used to cross-identify our sources with objects in the ONC catalog of H97 and to obtain plate transformations and J2000 coordinates of our sources, which are tied to the coordinates given in that paper, adjusted as follows. According to Hillenbrand (private communication), her coordinates require an adjustment of +1.5″ in right ascension and −0.3″ in declination to place them on the true J2000 system. This adjustment has been made to the positions reported in our Table 1. Of the 1575 stars in Hillenbrand's catalog, 1183 (75%) were matched with sources in our study. The average positional agreement was 0.3″. In a few cases there were differences in position

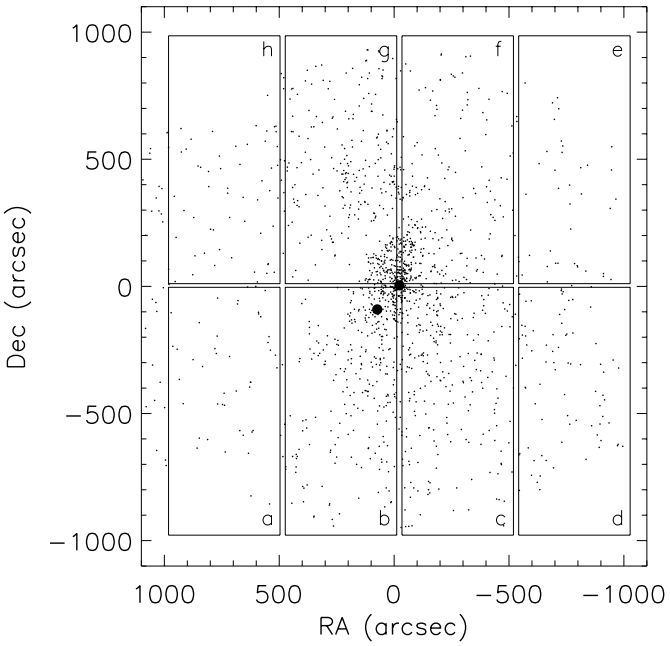

Fig. 1. The boxes represent the location of the 8 CCD chips which comprise the WFI. The lettering system is particular to this paper and does not conform to the usual WFI standard. Stars from the H97 catalog are plotted. θ^1 and θ^2 Ori are shown as larger dots.

which reached 2.1″, but these were quite rare. The stars in the Hillenbrand catalog which were not matched by us either fell in the gaps between the CCDs or beyond the boundaries of the frames, for the most part. A few objects near the center of the nebula may also have been missed as a result of background contaminination. Since our study extends to deeper limits and covers a slightly different area, we have sources which are not in the H97 catalog. Rather than use duplicate numbers for the same objects, we have chosen to adopt and extend the Hillenbrand numbering system by using numbers beginning at 10 000 for objects not in her catalog.

Since the seeing and pixel scale are excellent, these images are relatively uncrowded and aperture photometry is sufficient for obtaining accurate magnitudes in most cases. We chose to use it in this field where the nebular background is bright and highly structured because it is simple, accurate and straightforward. Admittedly, we did lose information on some crowded stars which profile fitting techniques might have preserved. The APPHOT task in IRAF was used to measure the brightness of each object within an aperture radius of 10 pixels (2.38″). The sky correction was calculated based on the median of an annulus with inner radius of 20 pixels (4.8″) and width of 10 pixels centered on the star. Since aperture photometry of stars with close companions is not reliable we have included, in Table 1, the separation, magnitude difference and identification number of the nearest neighbor to each object. In cases where the neighboring source is within the aperture, the photometry is obviously unreliable. Stars with neighbors less than 4″ distant have suspect photometry, although there may be little effect on the brighter star if the magnitude difference is large. The centering function in the APPHOT task was set to allow centering by up to 1″ during the photometry, so stars closer together than that

will always be measured at the brightness level of the brighter star. There were only 5 such pairs among our 1562 objects.

Establishing local flux standards is somewhat problematical, since almost all of the stars on the frames are PMS members of the cluster that are expected (and generally found) to be variables. The procedure adopted follows that outlined by Choi & Herbst (1996) which is to use the average magnitude of all of the stars on a frame initially as the flux standard and then to weed out the most obviously variable objects in iterative fashion. Eventually, a relatively stable set of stars can be found whose average magnitude from night to night serves as a flux standard. This procedure resulted in the identification of ∼10 stars on each of the 8 component CCD fields of the WFI that served to define the comparison magnitudes. The average external deviations of comparison stars was 0.007 mag or less in all cases. In the best cases, we achieved a precision of 0.005 mag which appears, therefore, to be the ultimate limit to the precision of our photometry. It is probably set by nightly errors in flat fielding. The differential magnitudes were shifted to a common photometric system for all 8 chips by correcting for the differences in average comparison magnitude between fields. The final magnitude system, which we call m_{816} was obtained by adding the offset between our instrumental magnitudes and the average Cousins I magnitude of the 1183 stars in common with H97. We have, therefore, placed our magnitudes roughly on the Cousins system, but we caution that a proper transformation, including a color term, has not been done, nor is it possible since we have observed through only a single filter.

For each star, we can calculate an average value of m_{816}. Figure 3 shows the difference between that value and the I magnitude reported by H97 for the 732 stars in common within the magnitude range $12 < m_{816} < 18$ which matched in position to 0.3″ or better and which had no companions within 5″. Most of the stars in Fig. 3 lie within a few tenths of a magnitude of the mean, although some scatter widely. The standard deviation of a point is 0.31 mag. and the mean absolute deviation is 0.17 mag. There is no evidence for a significant color term. We suspect that most of the scatter is real and caused by variability. This is supported by the fact that the standard deviation of the light curve (σ) from our photometry is positively correlated with the absolute value of $(I - m_{816})$. The existence and size of the scatter between our mean magnitude and the I magnitude reported by H97 should serve as a warning that masses and ages inferred for individual PMS stars from their location on the HR diagram may be seriously in error if based on only one or a few brightness measurements.

Figure 4 shows the relation between m_{816} and σ for stars in our sample. Brighter stars are saturated on at least some images which explains the increase in the minimum value of σ for stars brighter than 12.5 mag. It is evident from the figure that the majority of stars show only small variations and the lower envelope defines a minimum value of σ as a function of brightness that reflects the random errors of the photometry. In the interval $12.5 < m_{816} < 15.1$, the random error is at its lowest value, which is 0.005 mag. Beyond $m_{816} = 15.1$, the errors increase and that eventually limits our ability to study variability.

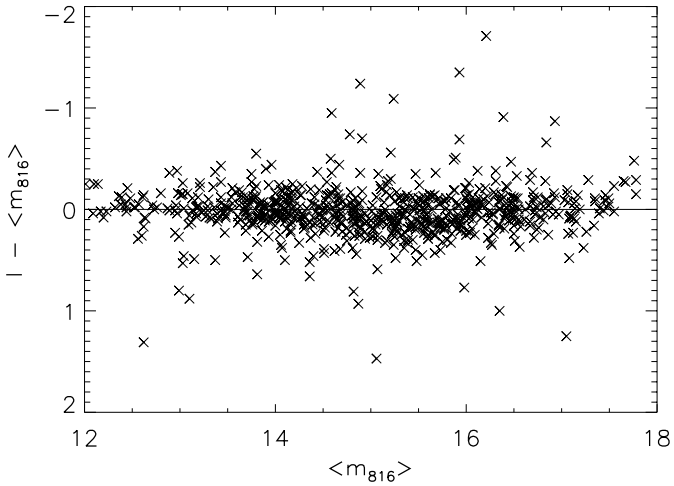

Fig. 3. Mean instrumental magnitude derived from our photometry versus the deviation of that magnitude from the Cousins I value reported by H97.

A reasonable fit to the lower envelope of errors is shown, given by the relationship

$$\sigma_{\rm limit} = 0.005 \quad \text{for } \sigma \leq 15.1,$$

$$\sigma_{\rm limit} = 0.005 \times 10^{0.4(m_{816}-15.1)} \quad \text{for } \sigma > 15.1.$$

Note that the periodic variables, which are shown as boxed points in Fig. 4, cluster close to but just above the minimum error line. This supports our claim that the photometric precision is better than 0.01 mag for stars brighter than $I = 16$. Otherwise, we would not have been able to detect the periodicity of these variables. Note also that there are few periodic variables fainter than 16th magnitude, especially among the low amlitude variables. This is also in agreement with our claim that the precision declines rapidly for fainter stars. Our failure to find many periodic stars fainter than $I = 16$ is almost certainly due to our precision, not to a real lack of periodicity among those objects, although we reiterate that the errors are just estimates.

Table 1, the full version of which is available electronically, summarizes our photometric results. For each star in the final sample, we give an ID number based on an extension of the H97 system (as described previously), a flag indicating if the star is has a binary designation in H97, the right ascension and declination on the J2000 system, the number of photometric measurements (N), m_{816}, σ, the "range" (defined here as the difference in median values of the upper 15% of measurements and the lower 15% of measurements), the period (in days) of any periodic stars, the separation (in arc-seconds) between a star and its nearest neighbor, the magnitude difference (Δm) between the star and its nearest neighbor, the ID number of the nearest neighbor (NID), the WFI chip on which the star is located, its number in our catalog (DNUM), and its x and y position on the reference image. As mentioned previously, photometry was obtained for all of the 2294 sources in our original list, and the adopted numbering system reflects that. However, since we have eliminated from Table 1 stars which are too faint

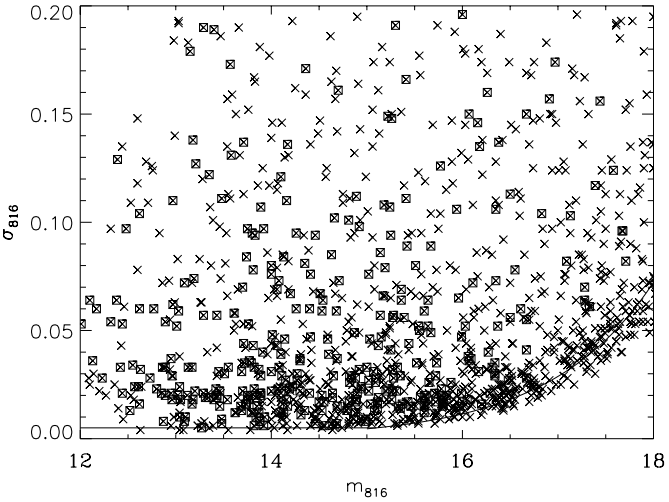

Fig. 4. The scatter in the data for each star, measured by σ, as a function of instrumental magnitude. Boxed points are periodic variables.

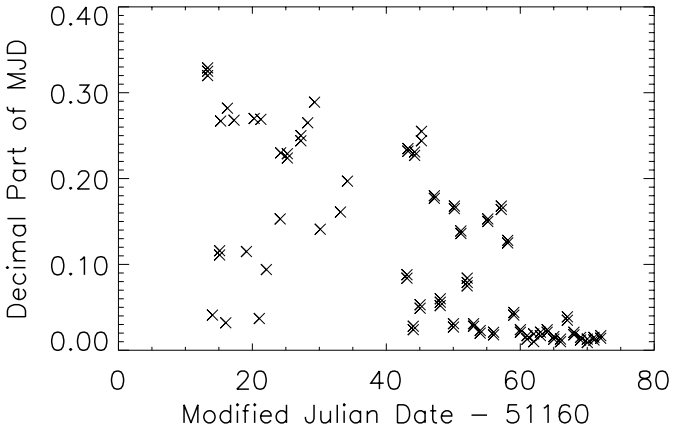

Fig. 5. Distribution of the times of observation, showing the time of night (expressed as a decimal fraction of a day) on the ordinate and the Modified Julian Date on the abscissa.

or too near the edges of the frames to yield consistently reliable photometric measurements only 1562 stars remain. Three of them (413, 10 141 and 10 797) would have been eliminated as being too close to the edge, but they turned out to be periodic stars, whose photometry was sufficiently reliable to report.

The distribution of times of observation during the night and the year are shown in Fig. 5. At the beginning of the observing period, in December and January, it was possible to observe the cluster at a wide range of times during the night and this was done in order to minimize the effects of aliasing in period determinations, as discussed below. Towards the end of February, the cluster was setting early in the night, and a wide range of observation times was not possible. It may also be seen from this figure that our coverage was nearly continuous except for a one week gap in the the middle.

Examples of some light curves are shown in Fig. 6 in order to illustrate the density and spacing of the data, the typical scatter of a comparison star and a few example light curves. Light curves for any or all of the objects in Table 1 are available from the first author by request. The stars chosen for display are ones which were found to be periodic and that accounts for the interesting patterns seen. Most of the stars, of course, cannot be identified as periodic simply by looking at their light curves and we turn now to a discussion of the identification of periodic variables.

3. Periodic variables

A periodogram analysis based on the method of Scargle (1982) was used to search for significant periodicity in all of the monitored stars, including those which were too faint or close to the frame edges to be listed in Table 1. This involves calculation of a normalized power (P_N) which must then be related to the false alarm probability (FAP). The problem with some standard methods for doing this (e.g. Horne & Baliunas 1986) is that they assume each magnitude measurement is independent of all others. This is not true when, for example, data are obtained at closely spaced intervals on some nights, because a typical time scale for significant TTS variation is ∼1 d. One approach is to average the data on short timescales, but this could make it harder to find very short period stars. Another approach, which we adopt here, is to use a Monte Carlo simulation to determine the relationship between P_N and FAP. A total of 1622 stars (including some fainter than the magnitude limit for inclusion in Table 1) with magnitude measurements on each of the 92 images were used to produce a random data set which preserved the correlations of the original data in the following way. The magnitude measurements and decimal parts of the MJD's were left untouched while the day numbers were randomly scrambled. This "randomized" data set was then searched for periods with the same techniques as used for the actual data. The highest power found in the randomized data set was 20.3 and 16 stars had peak powers exceeding 16.5. Based on that, we adopted a cutoff of $P_N = 16.5$ for identification of a star as periodic, roughly corresponding to a FAP of 1%. A few stars with powers exceeding this limit were rejected or had their adopted periods modified as discussed below. In total, 369 stars fulfilled our criteria to be considered periodic and 322 of them had $P_N > 19$, which we identify as corresponding to $FAP < 0.1\%$ by our Monte Carlo simulation. Table 2 lists the identification number, mean brightness, period, power and any possible alias of all 369 stars identified as periodic in this study.

A few of the rejected stars with powers exceeding 16.5 deserve some special mention. Most of these were removed from Table 2 because their periods were between 0.97 and 1.03 days (the dominant sampling frequency) and their phased light curves were not believable. A visual inspection of all of the light curves also revealed a few other stars which were rejected because their phased light curves were insufficiently convincing to warrant inclusion as periodic. None of these stars had periods reported by other authors. When in doubt, we left the star in Table 2. A sample of our phased light curves at different power levels is given in Figs. 7 to 10. The complete set of phased light curves is available electronically. It is interesting to note that the shortest period we found was 2/3 of a day, which was found for three stars. It is possible, of course, that these are actually beat periods or harmonics, but it is also rather

Table 1. Photometric data: full table available electronically at the CDS.

ID	Flag	RA(J2000)	Dec(J2000)	N	$< m816 >$	sigma	range	Per	Sep	magdif	NID	chip	dnum	X	Y
10 003	–	5:34:10.38	−5:19:38.7	92	18.12	0.079	0.22	0.00	19.4	0.62	10 001	*d*	174	1960.35	890.31
10 004	–	5:34:10.42	−5:10:20.8	92	14.67	0.006	0.02	0.00	6.8	4.49	10 005	*d*	173	1956.27	3237.48
10 005	–	5:34:10.55	−5:10:14.3	92	19.16	0.265	0.64	0.00	6.8	−4.49	10 004	*d*	172	1948.43	3264.57
10 007	–	5:34:10.89	−5:12:03.8	92	17.56	0.129	0.37	0.00	2.2	−0.29	10 008	*d*	170	1927.29	2804.02
10 008	–	5:34:10.97	−5:12:05.7	92	17.27	0.035	0.08	0.00	2.2	0.29	10 007	*d*	167	1922.51	2796.02
10 009	–	5:34:10.97	−5:18:18.4	92	17.42	0.038	0.11	0.00	29.9	1.72	10 021	*d*	169	1923.62	1228.28
10 012	–	5:34:11.10	−5:12:57.9	92	18.98	0.239	0.48	0.00	31.7	−1.53	10 000	*d*	165	1913.97	2576.43
10 013	–	5:34:11.22	−5:29:01.9	91	19.98	0.412	1.11	0.00	16.3	1.36	10 020	*e*	171	1910.89	2676.67
10 014	–	5:34:11.34	−5:15:54.3	92	19.24	0.216	0.57	0.00	9.0	2.39	10 006	*d*	164	1899.77	1834.29
3132	–	5:34:11.53	−5:30:19.7	92	15.80	0.015	0.04	0.00	9.5	6.06	10 016	*e*	170	1891.83	2349.66
3157	–	5:34:11.69	−5:33:55.8	92	15.06	0.008	0.02	0.00	1.4	0.01	10 015	*e*	168	1880.92	1441.26
10 015	–	5:34:11.69	−5:33:57.2	92	15.07	0.010	0.03	0.00	1.4	−0.01	3157	*e*	169	1880.96	1435.76
10 018	–	5:34:12.06	−5:35:23.3	92	18.52	0.106	0.29	0.00	26.8	−3.09	10 033	*e*	164	1857.94	1073.81
10 019	–	5:34:12.07	−5:24:19.2	92	15.25	0.031	0.05	0.00	30.7	1.86	10 038	*e*	165	1858.07	3864.56
10 021	–	5:34:12.38	−5:17:57.3	92	19.14	0.175	0.51	0.00	24.0	−2.73	3035	*d*	163	1835.15	1317.27
10 022	–	5:34:12.72	−5:15:31.5	92	18.30	0.092	0.25	0.00	15.6	1.24	10 035	*d*	162	1813.02	1930.45
10 023	–	5:34:12.74	−5:19:31.5	92	16.54	0.015	0.04	0.00	13.7	5.16	10 027	*d*	161	1812.52	920.65
10 025	–	5:34:12.88	−5:12:14.7	92	18.84	0.144	0.33	0.00	23.4	−0.54	10 039	*d*	160	1802.15	2758.39
3126	–	5:34:12.92	−5:28:48.1	92	13.20	0.022	0.06	8.46	7.9	5.05	10 028	*e*	161	1804.53	2734.75
3153	–	5:34:13.06	−5:33:48.4	92	16.40	0.225	0.72	0.00	5.6	−2.36	3156	*e*	160	1794.86	1472.47

close to the expected shortest period set by the critical rotation velocity expected for a PMS star in the ONC. The longest period was 22.2 days, for star 376, although the power is rather low.

There are 111 stars in our Table 2 which were also reported to be periodic by either SMMV or HRHC or both, and this information is included, along with the period adopted in this paper. A comparison between the periods found here and those previously reported is shown in Fig. 11. Crosses are used to represent stars observed at VVO as part of the studies summarized by HRHC (including ones reported independently by SMMV), while triangles refer to stars reported only by SMMV. Evidently, the large majority of our periods, 99/111, agree precisely with previous determinations. Furthermore, 11 of the 12 which disagree can be understood on the basis of two phenomena – harmonics and aliasing. The straight lines of slope 2 and 1/2 in Fig. 11 represent the loci of stars in which harmonics ("period doubling") must play a role. Figure 12 shows an excellent example of the phenomenon. Photometry of star 816 is phased with the shorter period, 1.77 days, in the top panel; this is where most of the power is found in the periodogram. It is clear, however, from the bottom panel that, in this case, twice that value (3.54 days) is the actual rotation period of the star since the photometric scatter is much less in this case. This star simply had a complex light curve at this epoch, clearly caused by two large spots at different longitudes. If we had not had data at other epochs, when a single spot dominated the light curve, we might easily have mistaken 1.77 d for the true rotation period of the star. While apparently not a widespread phenomenon, this sort of thing obviously does happen in a small percentage of cases (Fig. 11).

The "beat" phenomenon is also evidently responsible for some mistaken period determinations, as seen in Fig. 11. The problem is that there is a one day sampling interval in the data imposed by the fact that all the data were obtained from a single longitude, so a periodic phenomenon characterized by P will also generally yield beat periods, B, related to it by

$$\frac{1}{B} = \frac{1}{P} \pm 1.$$

Fortunately, in most cases it is possible to distinguish P from possible beat periods by the reduced scatter in the light curve. This is because the sampling interval is not really precisely one day or any other period (see Fig. 5). Normally, therefore, the true period has a higher peak in the periodogram representing a less scattered light curve. Sometimes, however, it is not possible to readily distinguish the true period from a possible alias. In these cases, we report a possible alias.

A nice example of what we take to be the beat phenomenon is the top star (g 022) in Fig. 6. During the second half of the monitoring time, when the data were obtained with a very regular interval of approximately one day (see Fig. 5) the star seems to have an ∼8−9d period. However, it is clear that during the earlier monitoring time, when there was greater spread in the intervals, the light curve becomes more scattered. When phased with a 1.13 d period, however, the light curve is much tighter at all times, and we take that to indicate that it is the true rotation period of the star. The beat period in this case is $(1–1/1.13)^{-1}$ or 8.69 d, and it is seen clearly in Fig. 6.

For definiteness, we have adopted the criterion that when two peaks in the periodogram agree in their power to within 5% we report them both, with the higher peak identified as the rotation period and the lower peak identified as a possible alias. 55 of our 369 stars with periods fell into this category. In most cases, we are confident that the higher peak will turn out to be the actual period, as Fig. 11 indicates. It is important, however, to keep the "aliasing" phenomenon in mind, especially

when considering the fastest rotators, since it appears to be easier to move power from low frequency to high in this data set. Stastically, aliasing should have little effect on the analysis; however, in studying individual stars and especially when trying to establish the extrema of the distributions including, for example, identifying the most rapidly rotating stars it is important to consider the possibility that a detected period may, in fact, be an alias.

There were twelve stars, altogether, which lay off the line of agreement in Fig. 11. Light curves from the various epochs for these stars were examined, phased with the different possible periods and judgements were made, based on the appearance of the light curves. In some cases it was possible to be reasonably certain about the period and, in other cases, it was not. Our comments on the individual cases are as follows:

- Star 149: at VVO a period of 2.83 d was found in one season and SMMV reported a period of 2.76 d, appearing to confirm it. The shorter period alias, 1.53 d, does not produce a very convincing light curve so we have adopted the longer period but this result must be considered somewhat uncertain.
- Star 167: at VVO a period of 1.40 d was found in only one season; the longer period of 3.43 d found here is preferred since the present data set is better.
- Star 192: a period of 4.52 d was found here; a period of 8.73 d was reported by SMMV. Can this be period doubling? It appears to be, although the case is not nearly so good as for star 816. We tentatively adopt $2 \times 4.52 = 9.04$ d for the star.
- Star 379: at VVO, periods of 5.65 and 5.59 d were found in two different seasons and this matches well with the period 5.54 d found here. However, SMMV reported a period of 11.3 d and argued that the light curve may have been double-peaked during the seasons in which it was observed at VVO. Inspection of the current light curve tends to support that idea, since it is not well defined with the 5.54 d period and does look as if it could be double-peaked. HRHC adopted the longer period and the current data tend to support that assignment, although the star remains a bit of a puzzle and an interesting object for further study.
- Star 381: this star has a single epoch period of 16.2 d determined at VVO. The light curve at the shorter period of 7.92 d found here is quite scattered and unconvincing. The amplitude is large. It could be another case of period doubling, since the periods are nearly integral multiples of one another. Here we adopt the longer period of 16.2 d.
- Star 710: this large amplitude variable has an average period of 7.59 d over many years at VVO and a period of 7.66 d according to SSMV. The light curve for the shorter alias (1.15 d) which had higher power here is unconvincing and there is no reason to think that the period assigned to this star on the basis of many seasons at VVO is incorrect. We adopt the longer period.
- Star 816: a period of 1.77 d was found here; a period of 3.60 d was reported by SMMV. This is a striking example of the period doubling phenomenon and was described in a previous paragraph and illustrated in Fig. 12. The correct period is clearly 3.54 d.
- Star 819: at VVO a period of 5.76 d was found in only one season; the shorter period of 1.21 d period found in this study is preferred here based on an examination of its light curve.
- Star 843: at VVO a period of 5.38 d was found at a single epoch. The present study, however, supports the result obtained by SMMV of 0.84 d.
- Star 880: at VVO a period of 3.51 d was found in only one season; the shorter period of 1.58 d is preferred here, again, on account of its light curve.
- Star 925: a period of 11.68 d is found here, which is rather inconsistent with the period reported by SMMV of 4.71 d. This is the only case where the periods do not match with either an harmonic or an alias. The power is fairly low also. We adopt the period of 11.68 d but it is uncertain.
- Star 984: the 8.44 d period obtained at VVO during a single season is probably an alias, since both the present study and SMMV find a period of 1.13 d and they are less susceptible to aliasing.

For convenience, we have brought together, in Table 3, all the periods which have been obtained for stars in the H97 catalog from this study, HRHC and SMMV – a total of 427 stars. We have not included periods detected only in Carpenter & Hillenbrand's (2001) infrared survey because, as they discuss, their data are very susceptible to the beat phenomenon. The nebulosity made it difficult for them to study stars in the ONC, as well. Obviously we have not included stars from Rebull (2001) since her study is limited to the flanking fields, not the ONC. We include in Table 3, the effective temperature, luminosity, mass and infrared excess of the star from H97. The mass is based on the models of D'Antona & Mazzitelli (1994), and the excess infrared emission, $\Delta(I-K)$, is from Hillenbrand et al. (1998). Before discussing the frequency distribution of the periodic variables as a function of mass, and its interpretation, we consider the general nature of the variability of the ONC stars in a bit more detail.

4. The nature of the variations

In this section we examine some general aspects of the variations of ONC stars which speak to the nature and causes of their variability. We also address the issue of whether the periodic stars are an unbiased sample of the full cluster in all respects. Our photometry is best suited for exploring the behavior of stars in the magnitude range $12.5 < m_{816} < 16$ that do not have companions closer than $5''$ – a total of 767 objects. We use the standard deviation, σ, to characterize the "degree" of variability since it is more robust than, say, peak-to-peak variations, which can be greatly distorted by a single accidental error. As a rule of thumb, we note that peak-to-peak variations are typically a factor of 5 larger than σ for the stars in this sample. Essentially all of our objects are variable at some level. The cumulative frequency distribution of stars with σ is shown in the upper left panel of Fig. 13. It is evident that about half of the total sample have $\sigma > 0.04$ mag, corresponding to

Table 2. Periodic stars detected during this study: full table available electronically at the CDS.

ID	*m*(816)	Per(d)	Power	Alias	*P*(HRHC)	*P*(SMMV)	*P*(Adopt)
3	13.02	3.43	38.0	0.00	0.00	3.37	3.43
4	12.66	8.46	43.4	0.00	0.00	8.26	8.46
7	15.69	1.53	24.2	0.00	0.00	0.00	1.53
10	13.80	8.66	31.4	0.00	0.00	0.00	8.66
11	15.16	1.73	33.5	0.00	0.00	0.00	1.73
13	15.52	5.46	30.7	0.00	0.00	0.00	5.46
15	14.07	9.56	21.5	0.00	0.00	9.65	9.56
17	13.41	3.14	23.2	0.00	0.00	0.00	3.14
20	13.68	0.67	17.4	0.00	0.00	0.00	0.67
21	13.74	12.06	43.7	0.00	0.00	0.00	12.06
24	13.52	14.41	22.8	0.00	0.00	0.00	14.41
25	15.20	2.28	25.7	0.00	0.00	0.00	2.28
33	14.65	1.50	41.0	0.00	0.00	0.00	1.50
35	12.77	5.99	30.7	1.20	0.00	6.00	5.99
36	14.41	2.72	17.8	0.00	0.00	0.00	2.72
37	13.12	8.27	21.5	0.00	0.00	0.00	8.27
40	14.40	9.81	34.7	1.11	0.00	0.00	9.81
70	15.13	1.50	25.2	0.00	0.00	0.00	1.50
76	13.46	6.40	29.7	0.00	6.33	0.00	6.33
77	13.70	1.50	43.8	0.00	1.50	1.50	1.50

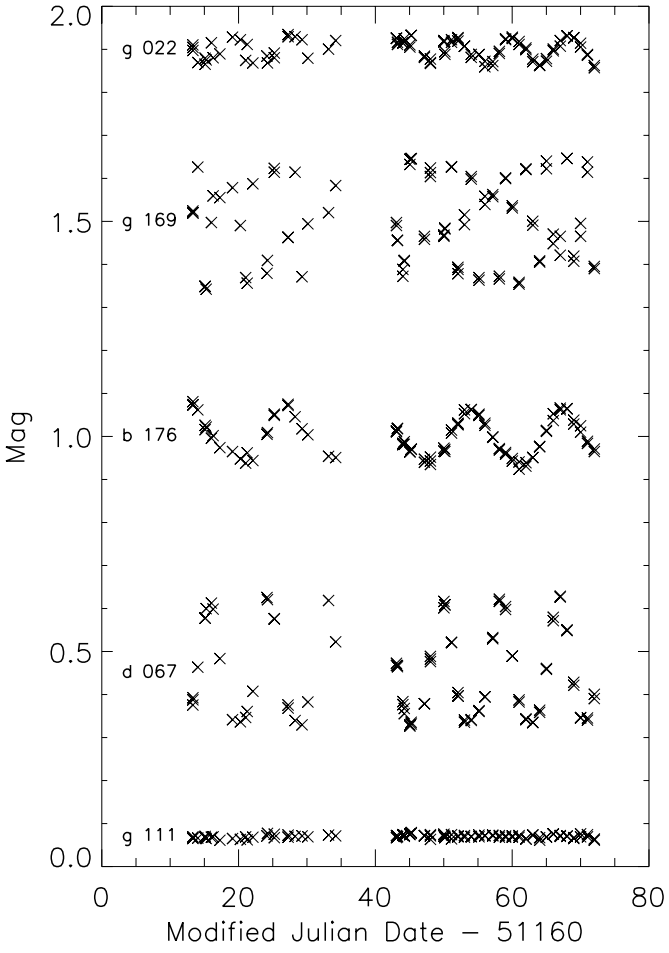

Fig. 6. Example light curves of a comparison star (g 111) and four periodic variables. Rotation periods are, in days, 8.46 (d 067), 13.9 (b 176), 2.85 (g 169) and 1.13 (g 022).

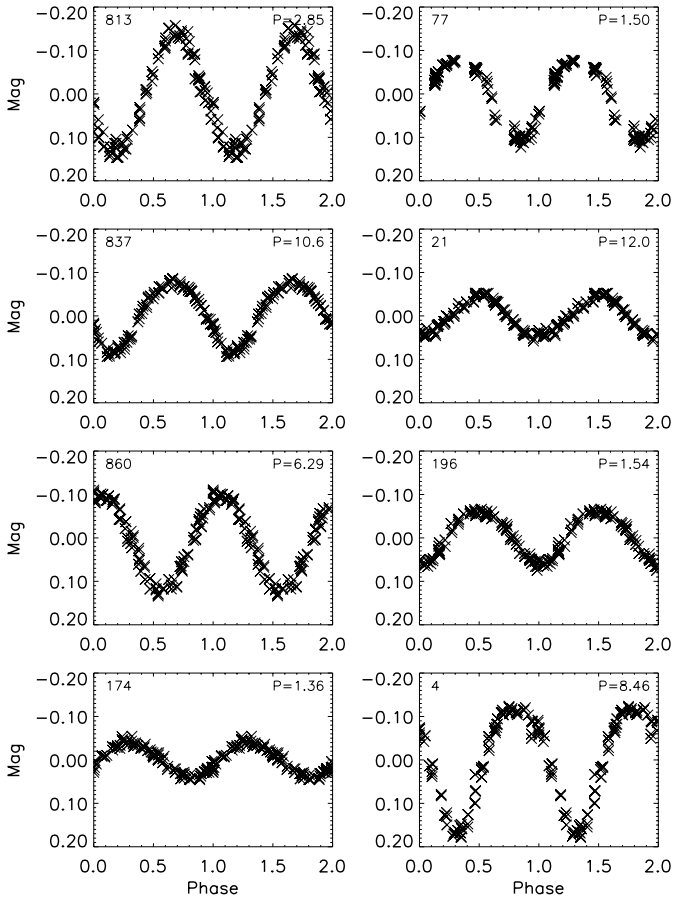

Fig. 7. Folded light curves for stars with normalized powers of ∼43. Each stars' identification number and period, in days, is given.

peak-to-peak amplitudes typically exceeding 0.2 mag. About 10% have very large variations, characterized by $\sigma > 0.2$ mag or peak-to-peak variations of 1 mag or more. It may also be seen that the periodic stars have a slightly different cumulative distribution from the total sample. Periodic variables make up 39% (297 stars) of the total sample in this magnitude range but they tend to be a bit more common among the lower amplitude variables. Considering only those stars with $\sigma < 0.1$ mag, we find that 46% of the sample is periodic. On the other hand, only 24% (48/197) of the stars with $\sigma > 0.1$ mag are found to be periodic.

To explore this difference between periodic and non-periodic stars further we show, in the upper right panel of Fig. 13, histograms of σ for the two types of variable separately. A two-sided Kolmogorov-Smirnov test (Press et al. 1992) indicates that the probability that the periodic and non-periodic samples are drawn from the same parent distribution is less than 3×10^{-5}. There are two explanations for this. First, the non-periodic sample contains many more stars with $\sigma < 0.01$ – i.e. essentially non-variables. Obviously, stars with such small variations will not easily yield periods. Perhaps more interesting, however, is the fact that we also see an excess of non-periodic stars among the larger amplitude variables – in particular, those with $\sigma > 0.1$. This is actually not surprising since it is precisely what is found among T Tauri stars in associations. Herbst et al. (1994) have shown, for example, that most WTTS

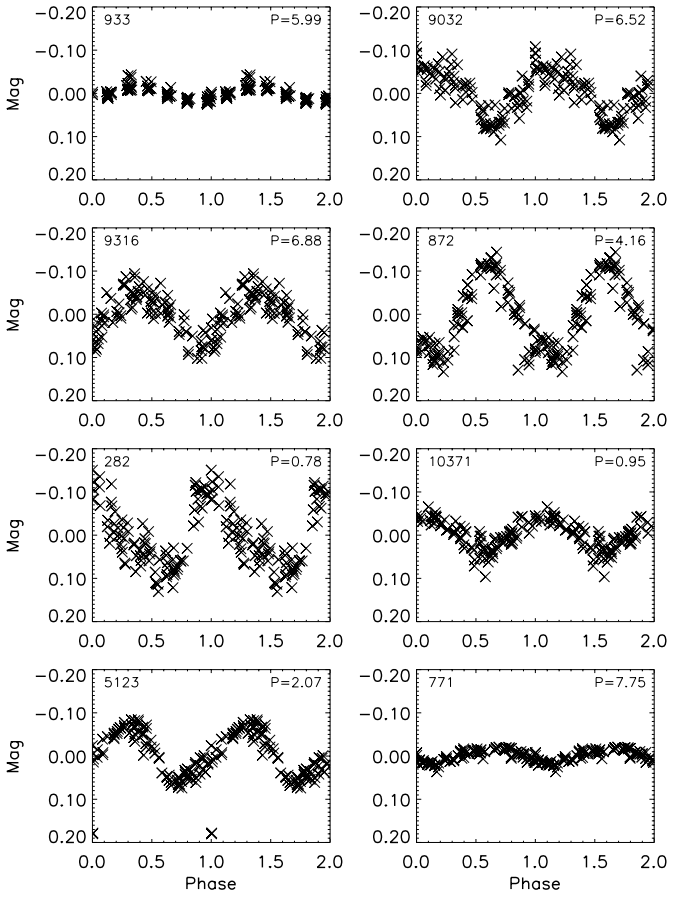

Fig. 8. Folded light curves for stars with normalized powers of ∼32.

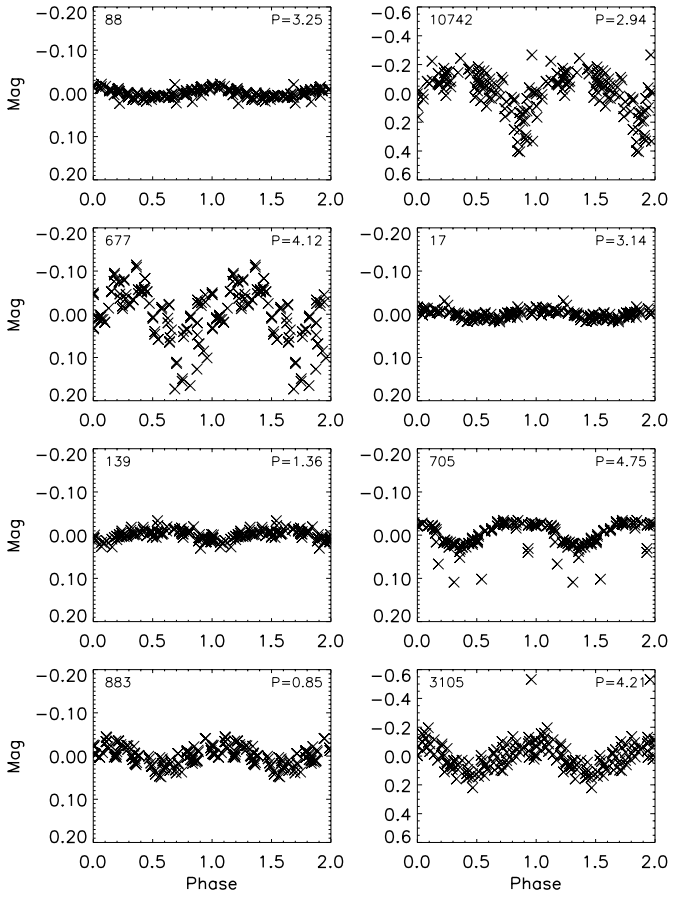

Fig. 9. Folded light curves for stars with normalized powers of ∼23.

in associations are periodic variables with peak-to-peak variations in I of less than 0.5 mag, while most CTTS are not periodic and often exhibit larger changes in brightness. It appears that the variables in the ONC mimic this behavior; periods are more commonly found among smaller (but not too small) amplitude variables. The similarity is more than just qualitative, since $\sigma = 0.1$ corresponds to a peak-to-peak variation of about 0.5 mag. As discussed by Herbst et al. (1994), the significance of this level of variabilty is that it is about the maximum one can attribute to cool spots on K and M stars.

To test these ideas further, we now enquire whether there is independent evidence from infrared data that low amplitude variables in the ONC tend to be WTTS while large amplitude variables tend to be CTTS. Figure 14 shows a plot of σ versus infrared excess emission, here measured by $\Delta(I - K)$ following Hillenbrand et al. (1998). This quantity, which is available for a large number of stars in our sample, is believed to be an indicator of circumstellar disk emission, *albeit* with large scatter (see below). A non-parametric, Spearman rank-order test (Press et al. 1992) confirms that σ and $\Delta(I - K)$ are correlated in our data at a very high confidence level. According to the Spearman test, the probability that such a good correlation would occur by chance in a data set this size is less than 10^{-27}. Stars with $\sigma < 0.03$ mag are clearly concentrated near $\Delta(I - K) = 0$, indicating that they lack evidence for a circumstellar disk and may, therefore, be considered WTTS according to the usual definitions. By contrast, stars with larger amounts of variability have, on average, significant positive values of $\Delta(I - K)$ indicative of the presence of an accretion disk. Commonly, the criterion of $\Delta(I - K) > 0.3$ mag is used to classify a star as a CTTS. As σ increases, the fraction of CTTS to WTTS according to that criterion also increases, rather dramatically. As Fig. 14 makes clear, there is no distinction in these results between periodic and non-periodic stars. The lower two panels of Fig. 13 also show that there is no significant difference in infrared excess emission or in $v \sin i$ between the periodic and non-periodic stars. The latter result is consistent with what was reported by RHM on the basis of a similar data set.

We conclude, on the basis of this discussion, that our data in the ONC provide substantial new support for the canonical view of PMS variability. Namely, we find that WTTS tend to be smaller amplitude variables than CTTS and are more commonly found to be periodic, while large amplitude variables are less likely to be found periodic and more likely to have infrared excesses characteristic of CTTS. All of this is consistent with the view that ONC cluster variables are not fundamentally different from TTS in associations. A similar result was recently found for TTS in the young cluster IC 348 by Herbst et al. (2001). Like their better-studied counterparts in associations, we may expect that the variations of the lower amplitude cluster variables are primarily a result of large, relatively stable, cool spots on their surfaces which are the magnetic footprints in their photospheres of the strong dipole field commonly invoked

Table 3. A comprehensive list of periods for stars in the H97 Catalog from this paper, HRHC and SMMV. The full table is available electronically at the CDS.

ID	Per (d)	Source	Log$T$	Log$L$	Mass	$\Delta(I-K)$
3	3.43		3.580	0.24	0.27	0.55
4	8.46		3.661	0.56	0.80	0.57
7	1.53		3.500	−1.09	0.13	0.06
10	8.66		3.633	0.23	0.59	0.67
11	1.73		3.465	−0.62	0.11	−0.50
13	5.46		3.518	−0.92	0.19	−0.21
15	9.56		3.562	−0.18	0.30	0.11
17	3.14		3.509	−0.20	0.16	0.10
20	0.67		3.518	−0.40	0.20	0.10
21	12.06		−9.999	−9.99	−9.99	−9.99
24	14.41		3.562	−0.31	0.34	0.08
25	2.28		3.500	−0.88	0.14	0.52
33	1.50		−9.999	−9.99	−9.99	−9.99
35	5.99		−9.999	−9.99	−9.99	−9.99
36	2.72		3.526	−0.30	0.21	0.46
37	8.27		3.679	0.14	1.15	0.62
39	5.51	SMMV	3.526	−0.63	0.23	0.14
40	9.81		3.518	−0.57	0.21	0.12
63	4.10	SMMV	3.623	0.26	0.50	0.20
65	7.39	HRHC	3.580	−0.24	0.39	0.50
70	1.50		3.494	−0.49	0.14	−0.35
73	2.23	SMMV	3.562	−0.59	0.41	1.65
75	3.45	HRHC	3.695	0.89	1.50	0.09
76	6.33		3.509	−0.23	0.16	0.16
77	1.50		3.580	−0.21	0.38	0.42
79	2.14		3.500	−0.98	0.14	0.37
81	4.41		3.580	−0.01	0.32	0.30
83	7.72	HRHC	3.544	−0.29	0.26	0.37
84	2.45		3.526	−0.70	0.23	−0.08
87	3.11		3.518	−0.67	0.20	0.12
88	3.25		3.555	0.04	0.24	−9.99
91	17.08		3.509	−0.24	0.16	−0.06
93	5.89		3.500	−1.02	0.14	−9.99
94	4.75		3.535	0.04	0.19	−0.60
95	1.31	SMMV	3.591	−0.12	0.40	0.22
98	2.34		3.509	−0.51	0.18	0.17

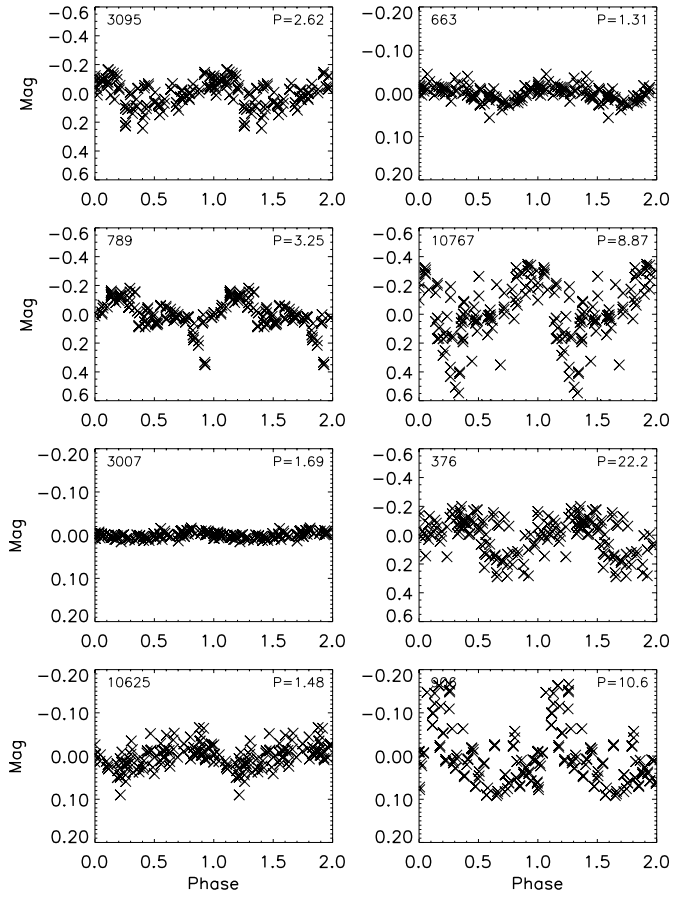

Fig. 10. Folded light curves for stars with normalized powers of 16.5–16.9.

in magnetospheric models of TTS. An increasing proportion of the larger amplitude stars have an overlying irregular variability caused by hot spots which come and go on time scales comparable to or less than a rotation period and make it ultimately less likely, if not impossible, to find periodicity. These changing hot spots are presumably a result of unsteady accretion, channeled into funnel flows from circumstellar disks.

We further conclude that the set of periodic stars is an only slightly biased sample of the full cluster with respect to rotation and disk properties. It is deficient in very low-amplitude (essentially non-variable) stars which are unlikely to have disks. It is also deficient in large amplitude (irregular) variables which, statistically speaking, have infrared excess emission and may, therefore, be regarded as CTTS. Fortunately, these two biases are in opposite directions when it comes to disk and, presumably, rotation properties. Perhaps for this reason or perhaps because the deficiencies are rather small to begin with, there is no noticeable effect on the distributions of $\Delta(I-K)$ or $v \sin i$, as the bottom panels of Fig. 13 show. We address, in Sect. 6, the estimation of a small quantitative bias correction factor that can be employed in any further analysis and conclude that is ∼15% or less.

5. Period distributions as a function of mass and infrared excess

As discussed by HRHC, and in Paper I, the rotation properties of ONC stars show a strong dependence on mass. The dividing line between two distinctly different populations is at about 0.25 $M_\odot$ if the models of D'Antona and Mazzitelli (1994) are used to infer mass from location on an HR diagram, or as high as 0.5 $M_\odot$, if other models are used (e.g. Palla & Stahler 1999; Baraffe et al. 1999). For definiteness, following H97, we adopt the D'Antona and Mazzitelli results for this discussion. This corresponds to a spectral class of ∼M2 or a $\log T = 3.544$. Figure 15 shows that the brighter, more massive stars in the ONC have a clearly bimodal distribution, as discovered by Attridge & Herbst (1992) about a decade ago. While there was some controversy about this result when the sample size was smaller (see SMMV and HRHC), it surely must now be regarded as indisputable. What is also certainly clear from Fig. 15 is that the fainter, lower mass stars in the ONC, do not

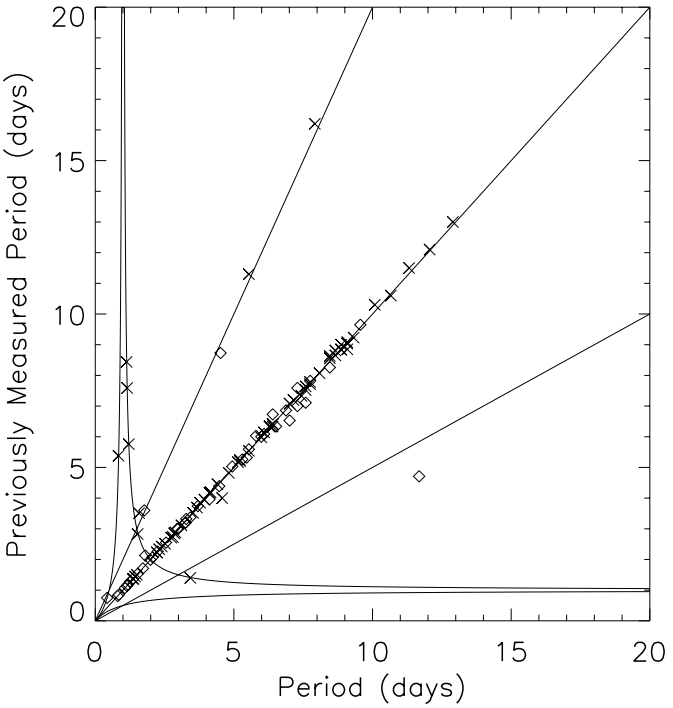

Fig. 11. A comparison between rotation periods determined in this study plotted on the abscissa and those reported by HRHC (crosses) and by SMMV (diamonds), plotted on the ordinate. The straight lines represent factors of 2 difference (harmonics) and the curved lines are the loci of beat periods with respect to the one day sampling interval.

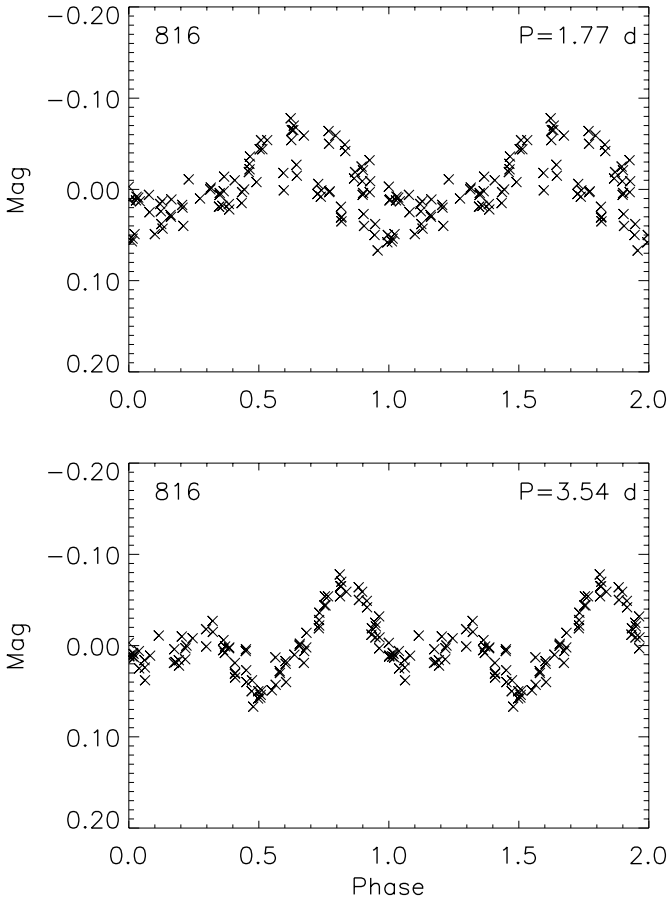

Fig. 12. Data for star 816 plotted with two periods. The periodogram analysis yielded $P = 1.77$ d during this epoch, but it is clear that the star's actual rotation period is 3.54 d and that two spots were present during the current epoch.

share the bimodal character of the period distribution. In particular, there is only a "tail" of slow rotators in that sample, and nothing like the second peak near 8 days which is so prominent in the case of the higher mass stars. What can account for this fascinating structure in the period distribution of the higher mass stars and why is there a dichotomy of behaviors between the higher and lower mass stars? We discuss the bimodal distribution first.

The original proposal by Attridge & Herbst (1992), which was developed at greater length by Choi & Herbst (1996), was that magnetic coupling between the star and the disk was "locking" the rotation of some stars to ∼8 day periods. This interpretation was based on the suggestions and models of Camenzind (1990), Königl (1991), Shu et al. (1994) and Ostriker & Shu (1995). Disk-locking nicely accounted for the longer period peak in the distribution; the shorter period peak is simply a result of the binning process when period is used (as opposed to angular velocity, for example). It has no physical significance. When stars are released from their magnetic lock they spin up as they contract, conserving angular momentum and moving into a period bin at 0–2 days. To justify this interpretation one would ideally like to show that slowly rotating stars do, indeed, tend to have disks around them while rapidly rotating stars do not. Edwards et al. (1993) and Bouvier et al. (1993) discussed the first such evidence in support of the picture, which was augmented by Choi & Herbst (1996) and, most recently, by HRHC. Evidence to the contrary, however, was reported by SMMV who claimed, in particular, to find no correlation between rotation and infrared properties indicative of circumstellar disks.

We reexamine the issue here, using the greatly expanded data set on rotation now available from this study. As in Sect. 4, we measure circumstellar emission by $\Delta(I-K)$ from Hillenbrand et al. (1998), because it is the only such measure that is currently available for a large number of ONC stars. Despite the inherent problems with this, reviewed below, we find that it is adequate for our purposes. The good correlation between $\Delta(I-K)$ and σ shown in Fig. 14 gives us additional confidence in its value as an indicator of the presence of an inner disk. Figure 16 shows $\Delta(I-K)$ plotted against the angular velocity ($\omega = 2\pi/P$) in radians/d for stars in Table 3. (Angular velocity is better suited to this discussion than rotation period, since it alleviates the crowding of rapid rotators in the figures and is directly proportional to the most important physical parameter, angular momentum.) Solid circles denote higher mass stars ($M > 0.25\ M_{\odot}$) and crosses denote lower mass stars. Evidently, in spite of all the caveats to be discussed, a clear correlation between rotation and infrared excess emission, measured by $\Delta(I-K)$ is seen in our data. To test the significance of the correlation, we have again applied the Spearman rank-order correlation test (e.g. Press et al. 1992), which is nonparametric and widely used. The correlation coefficient is 0.36, indicative of the wide scatter in the points at any value of ω but the significance level of the correlation is very high. According

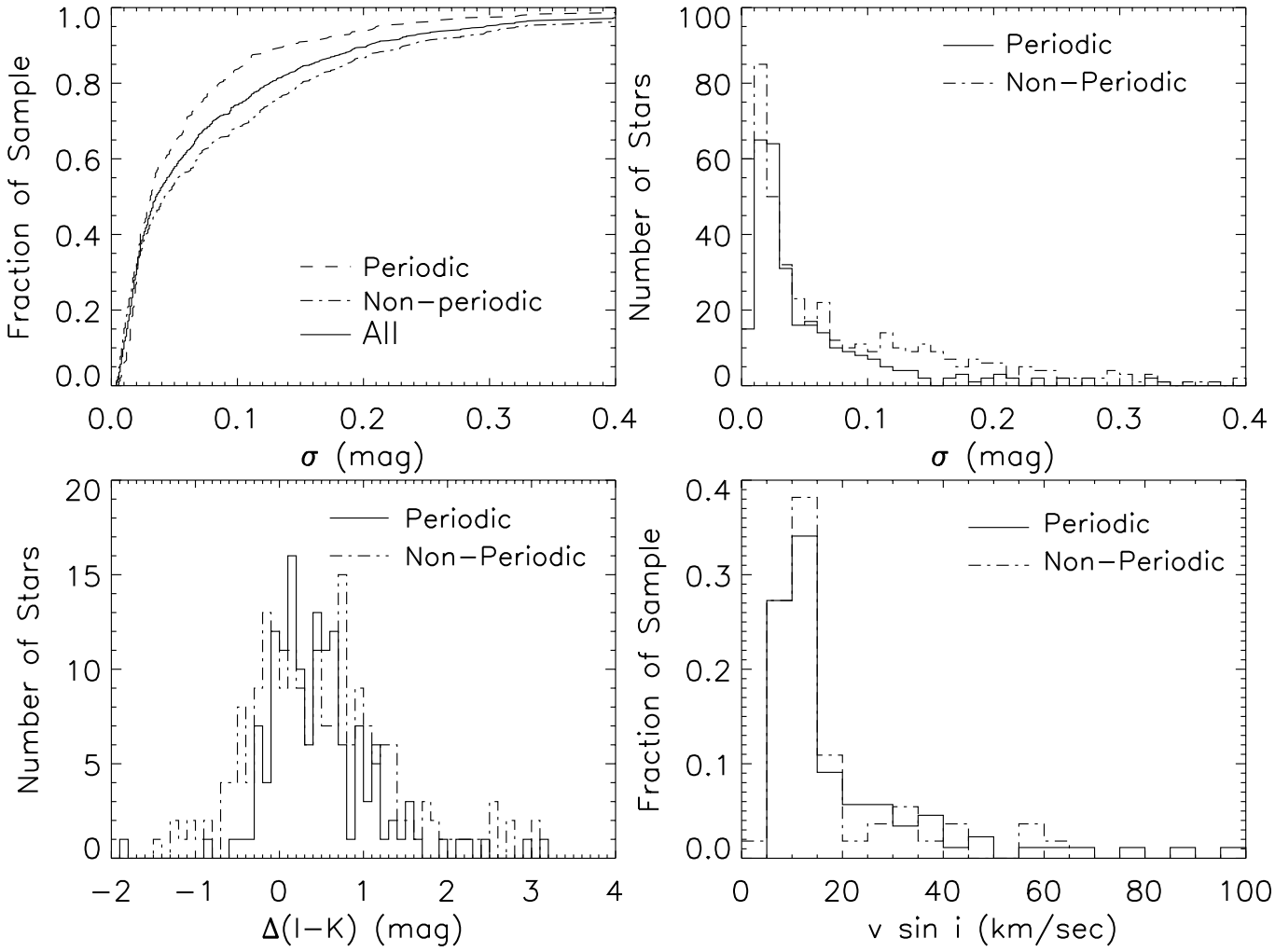

Fig. 13. a) The upper left panel shows the cumulative distribution of σ for uncrowded stars in the magnitude range 12.5–16. A slightly larger fraction of the stars with small amplitude variations are found to be periodic. There are 767 total stars, of which 297 are periodic in this sample. **b)** The upper right panel shows a histogram of σ for the periodic (solid line) and non-periodic (dashed line) stars respectively. It may be seen that the distributions are similar except for a sharper decline in periodic stars that begins at about $\sigma = 0.1$ mag. A Kolmogorov-Smirnov test indicates that the distributions are significantly different. We suggest that larger amplitude stars are less often found to be periodic because they have more irregular variability due to unsteady accretion from a circumstellar disk. **c)** The lower left panel shows a histogram of $\Delta(I-K)$ values for periodic and non-periodic stars. There is no significant difference in the distributions. **d)** The lower right panel shows a similar comparison of the periodic and non-periodic samples in terms of v sin i from RHM. Once again, there is no significant difference in the distributions, confirming the result reported by RHM.

to the Spearman test the probability of obtaining as good a correlation in a data set of this size by pure chance is approximately 3×10^{-11}. There is a small difference in the distributions of the higher and lower mass stars on Fig. 16, which will be discussed further below. However the correlation exists for each mass range separately with an obviously reduced, but still extremely high significance level.

Another way of assessing the statistical significance of a relationship between rotation and infrared excess emission, which may be more familiar to many readers, is to calculate the mean value of $\Delta(I-K)$ for slow and rapid rotators respectively. Guided by Fig. 16, we divide the sample into stars with $\omega < 1$ (i.e. rotation period longer than 6.28 days) and stars with $\omega > 2$ (i.e. rotation period shorter than 3.14 days). The slowly rotating sample has 118 stars and a mean value of $\Delta(I-K)$ of 0.55 ± 0.05 mag. In other words, this group has a clear indication (at roughly the 11σ level) of an infrared excess indicative of circumstellar emission. The mean value well exceeds the commonly adopted criterion of $\Delta(I-K) = 0.3$ mag to be "certain" that a disk is present. Statistically speaking, there is clear evidence that our slowly rotating stars still have (inner) disks. This result may be compared with the rapidly rotating sample, which has 121 members. In this case we find the mean value of $\Delta(I-K)$ to be 0.17 ± 0.05 mag, significantly less than for the rapid rotators and only about 3σ above the zero level indicative of no circumstellar emission. In fact, the mean value falls well below the commonly adopted threshhold value of 0.3, indicative of the "certain" presence of a disk. Figure 17 shows

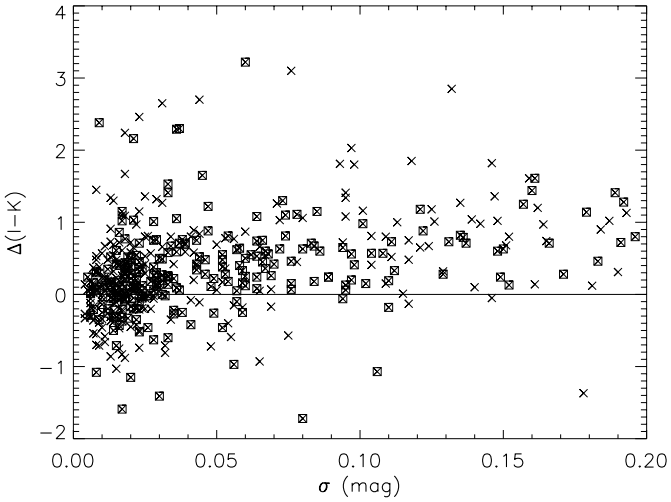

Fig. 14. The degree variability, measured by σ, is correlated with infrared excess emission, measured by $\Delta(I-K)$ from Hillenbrand et al. (1998). Low amplitude variables tend to have small or zero infrared excess emission and are identified as WTTS. Larger amplitude variables tend to have infrared excess emssion. Although there is considerable scatter in $\Delta(I-K)$, for reasons discussed in the text, the correlation is clear and supports the canoncial interpretation of the variability of PMS stars. Boxed points represent periodic stars and they show the same trend as the non-periodic variables.

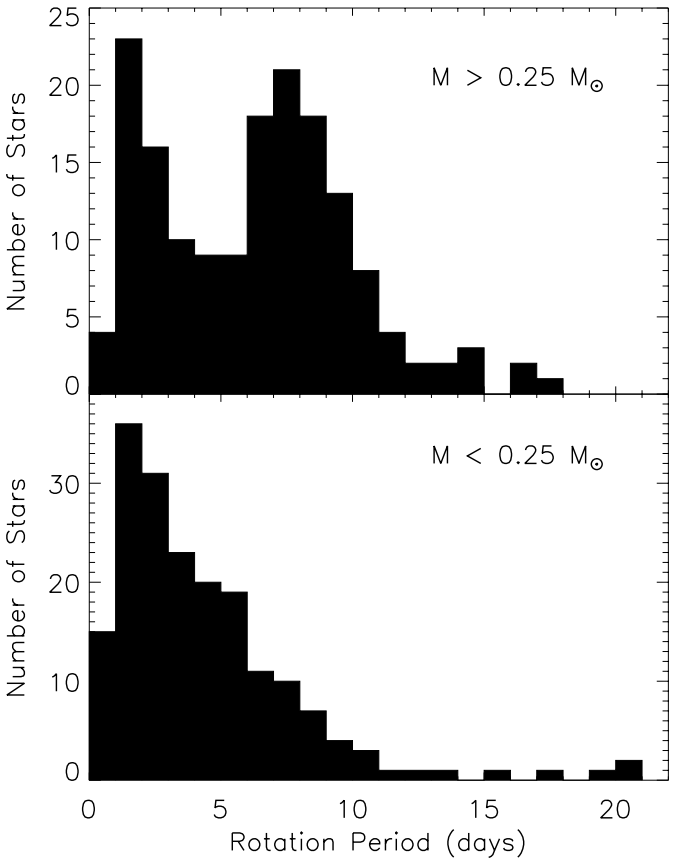

Fig. 15. Histograms showing the period distribution for ONC stars with masses exceeding 0.25 $M_\odot$ (top panel; mass estimate based on the models of D'Antona & Mazzitelli 1994) and with masses less than 0.25 $M_\odot$ (bottom panel). This is nearly equivalent to dividing the sample by spectral type at M2, or by effective temperature at $\log T = 3.544$. It is clear that the higher mass (hotter) stars have a bimodal period distribution and that the lower mass (cooler) stars spin faster, in general, and have a unimodal distribution.

histograms for the two samples and their difference is clear. A two-sided Kolmogorov-Smirnov test confirms the result for the means: the chance that slow and rapid rotators have the same distributions of infrared excess is less than 3×10^{-8}. We conclude that our data clearly support the view that the presence of an infrared excess, indicative of a circumstellar disk, is associated with relatively slow rotation of PMS stars in the ONC.

Although the connection between rotation and infrared emission is statistically significant at a high level, there is still a great deal of scatter in Fig. 16 which deserves further comment. Some of it may be due to observational errors, but some of it may be real and contain information about the angular momentum evolution of ONC stars. We begin by noting potential sources of observational error. Infrared variability (see Carpenter & Hillenbrand 2001), optical variability (see Figs. 3 and 13), errors in spectral classification, possible reddening law anomalies, disk orientations, radiative transfer effects, non-planar dust, central holes and probably other factors can all conspire to make $\Delta(I-K)$ a less than perfect indicator of the presence of a disk (e.g. Hillenbrand et al. 1998). However, even if a totally reliable disk indicator were available and disk-locking were operative, it is clear that we should not expect to find a perfect correlation between period and infrared excess emission in the ONC. One reason is that rotation does not respond instantaneously to changes in the structure or even the presence of a disk. We now consider this important issue in a bit more detail.

How long would it take an ONC star to react to the loss of its disk and spin up significantly? This is quite easy to answer assuming conservation of angular momentum, $J = I\omega$, where I is the moment of inertia and is given by $I = k^2R^2M$ and k is the normalized radius of gyration (0.44 for a fully convective PMS star). On their Hayashi tracks, stars evolve at roughly constant effective temperature and, since they derive their luminosity almost entirely by contracting, it is easy to show that $R \propto t^{-\frac{1}{3}}$ (see Sect. 6). Conservation of angular momentum, therefore, requires that $P \propto R^2 \propto t^{-\frac{2}{3}}$. If the current age of the ONC stars is $t_{\rm cluster}$ (i.e. the age of the cluster), and we take the disk-locked period to be 8 days, then the time needed to spin up to, say, half that period for a star released from its disk lock today is $2.8t_{\rm cluster}$ or, roughly 2–3 million years. Clearly this is much longer than the time for disk dissipation as currently measured. For example, in the ONC, the time scale for evaporation of the disks may currently be as short as $\sim 10^5$ y (O'Dell 2001 and references therein). Many stars are obviously in the process of losing their disks and others have presumably lost them recently. There should be a population of stars, therefore, which currently have no disks and cannot be disk-locked but have, nonetheless, not yet had time to spin up appreciably. In our view, this is the most likely explanation for a set of slowly rotating stars without infrared excess emission that contribute to the scatter in Fig. 16.

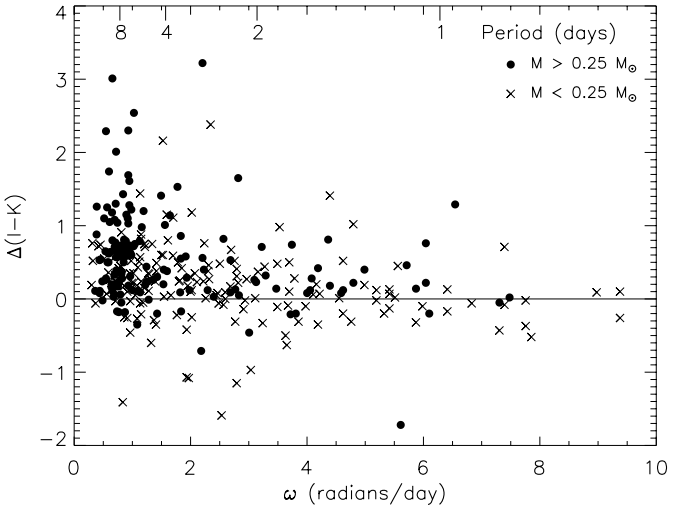

Fig. 16. Angular velocity (ω) is correlated with infrared excess from Hillenbrand et al. (1998), such that slow rotators have a greater probability of having IR excesses. Although the scatter is large, for reasons discussed in the text, the correlation is significant at a very high level (less than 10^{-10} chance that the quantities are not correlated) according to a standard, non-parametric (Spearman) test.

Another aspect of this issue has recently been discussed by Hartmann (2002) who points out that a disk can only transfer angular momentum to and from a star at a finite rate. His analysis of the time scales involved indicates that it is possible that disk locking has not yet had time to operate on some stars in the ONC, depending on their ages, accretion rates and "initial" angular velocities. This could explain, for example, how some rapidly rotating stars might nonetheless show evidence for circumstellar disk emission. Of course, if it were generally true of the more massive ($M > 0.25\ M_{\odot}$) ONC stars that they had not yet had time to be influenced by their disks, then the bimodal distribution and the correlation of rotation with infrared excess could not be explained as a result of disk-locking. Hartmann's analysis suggests that most stars in the ONC would indeed have had time to become locked to their disks if their initial angular velocity is not too large. Applying his equation (8) to the stars with 8 day periods and adopting the fiducial values of 0.5 $M_{\odot}$ for the mass and $10^{-8}\ M_{\odot}\ \mathrm{y}^{-1}$ for the accretion rate suggests a disk braking time of about 2×10^5 y. Since the mass accretion rate must have been higher at the earlier PMS (or proto-star) stage and since the disk-locking time scale depends inversely on it, the ONC stars in the relevant mass range should have had sufficient time to become locked to their disks unless their initial angular velocities are several times larger than currently observed. A detailed analysis of this possibility is beyond the scope of the present paper but we return to some discussion of it in Sect. 6.

To summarize, we have found in this expanded data set that the original discoveries by Attridge & Herbst (1992), Bouvier et al. (1993) and Edwards et al (1993) of a bimodal period distribution and a correlation of rotation with circumstellar disk emission, are confirmed. The bimodal period distribution is further shown now to apply only to the more massive ($M > 0.25\ M_{\odot}$) stars. The evidence in favor of accretion disks as an important factor in regulating the rotation of solar-like stars in young clusters now appears undeniable. To the authors' knowledge there is no competing mechanism which can account for these results in even a qualitative manner. The principal objections to the idea of disk-locking, raised by SMMV, have now been addressed. It remains to explain the difference between the rotation of higher and lower mass stars and to exploit the observed rotation distribution to gain insight into the time scales for transfer of angular momentum and for disruption of disks. In the next section we consider a simple, commonly adopted model which, if applicable, provides information on how long stars in the ONC remain locked to their disks. We also consider how this simple model can be extended to account for the mass dependence of rotation in the cluster.

6. Discussion

The results of the previous section suggest that disks are involved in regulating the rotation of stars in the ONC and must in some way account for the bimodal period distribution and the dependence of rotation on mass. The "canonical" explanation for how this is done is to assume that disk-locking occurs in the proto-star or early PMS stage and maintains the stars at a roughly constant angular velocity ($\omega \sim 1$ rad d^{-1}) until the disk lock is broken. After that, stars spin up as they contract, conserving angular momentum. The distribution of disk-locking times (as a function of mass) then accounts for the distribution of observed rotation periods. A detailed model based on this idea is presented below which allows us to place limits on the disk-locking times.

Before proceeding to explore this model, however, we note another possible scenario to account for the bimodal period distribution and correlation of rotation with infrared excess. Namely, it is possible that during the proto-star or early PMS evolutionary phase most or all stars spin up to angular velocities much larger than 1 (i.e. rotation periods much less than 6 days.) The effect of disk-locking, then, will be to slow some of them down to the observed ~8 day period. These will, of course, be stars with the highest accretion rates, accounting for the observed correlation between rotation and infrared excess. An attraction of this hypothesis is that it predicts a sense for the IR-rotation correlation that agrees with the data. The simplest form of the disk-locking hypothesis, on the other hand, predicts that larger IR excess should correlate with *shorter* periods among the disk-locked sample, because higher accretion rates lead to locking points which are closer to the star. A detailed model, based on this hypothesis or on some combination of these scenarios, is beyond the scope of the present paper, but would be an interesting exercise.

Here we employ the observed period distribution to estimate the characteristic time (e.g. half-life) during which an ONC star remains locked to its disk. We assume that a solar-like star becomes locked during the proto-star or early PMS phase (i.e. roughly at the birth line). The angular velocity during the locked phase, ω_{lock}, is not necessarily a constant. It can evolve over time in response to changes in the mass accretion rate or magnetic properties of the star. For our purposes, ω_{lock} is simply the value of the angular velocity when the disk no

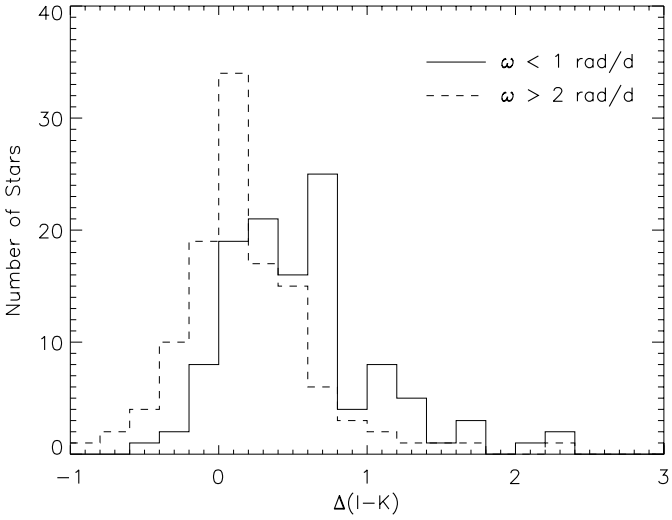

Fig. 17. The distributions of $\Delta(I-K)$ for slow and rapid rotators, respectively, regardless of mass. Clearly, the slow rotators are more likely to have an infrared excess, indicative of a disk, than are the rapid rotators. The probability that these two distributions were drawn from the same parent population is less than 3×10^{-8} according to a two-sided Kolmogorov-Smirnov test. This figure supports the view that disks tend to slow the rotation of PMS stars.

longer influences rotation (i.e. at the point where angular momentum conservation applies). After a time, $t = t_{\rm lock}$, the star is released from its disk (probably because the gas disk has been dissipated by evaporation or accretion or both) and, from that point forward, the star conserves angular momentum. Under these assumptions it is easy to calculate how long ago any particular star was released from its lock, knowing only its current angular velocity, ω, and $\omega_{\rm lock}$. While $\omega_{\rm lock}$ is not known with certainty for any particular star, its current distribution is known from observations of disk-locked stars. Therefore, for a cluster of stars like the ONC it is possible to reconstruct, in a statistical sense, the history of disk-unlocking, a task with which we now proceed.

Our analysis is based on some underlying assumptions which are, perhaps, worth noting explicitly at the outset. First, we assume that the stars are rigid rotators such that there are no radial or latitudinal variations of ω. Obviously, there is little observational or theoretical justification for this and the Sun and Jupiter are excellent counter-examples. However, in the absence of any information on how ω varies with latitude or depth in a PMS star, or even what latitude we are sampling by studying spot-induced photometric variations, we have little choice in the matter. We simply note that multi-epoch studies stretching over as much as a decade have failed to produce any clear evidence for variations in the rotation period of any PMS star that might be ascribed to latitudinal variations in ω. We further note that PMS stars are believed to be fully convective so that the transport of angular momentum within the stellar interior should be efficient. We also assume that the ONC stars can be represented as a homologous set of polytropes of index 1.5 so that the normalized radius of gyration, k, has the value 0.44. This is supported by detailed models of PMS stars (e.g. Krishnamurthi et al. 1997). With these assumptions, we may write

$$J = k^2 R^2 M\omega = \frac{2\pi k^2 R^2 M}{P}. \quad (1)$$

Since P is known in Eq. (1) much more precisely than R for PMS stars, the largest uncertainty in interpreting the rotation data is, actually, the stellar radii, not their angular velocities. It is also apparent that the specific angular momentum, $j = J/M$, will be better constrained by the data than J itself (see Paper I for more discussion of this).

It is well known (e.g. Hayashi 1965), that solar-like stars in their early PMS phase contract along nearly vertical tracks in the HR diagram, corresponding to nearly constant effective temperature ($T_{\rm e}$). Since their luminosity is generated almost entirely by gravitational contraction, we may write, using the homologous polytrope approximation, that

$$L = 4\pi R^2 \sigma T_{\rm e}^4 = \frac{{\rm d}(\frac{3GM^2}{3.5R})}{{\rm d}t} \quad (2)$$

which, for constant M and $T_{\rm e}$ yields

$$\frac{{\rm d}R}{{\rm d}t} = \frac{14\pi R^4 \sigma T_{\rm e}^4}{3GM^2}. \quad (3)$$

In this case, $t = 0$ corresponds to infinite radius (i.e. the beginning of the star formation process), and we obtain the usual result that $R \propto t^{-\frac{1}{3}}$. Note that this simple analysis neglects the existence of a proto-stellar stage of free-fall collapse. However, that simplification is acceptable in the present context because the proto-star phase is short compared with the relevant time scales of interest here, and is sufficiently well approximated by the time taken to collapse from infinite radius to the birthline radius. The ratio of radii, at any two times during the PMS phase is specified by the proportionality. In particular, if the radius at the time that the star loses its disk-lock is called $R_{\rm lock}$ and the radius today (i.e. at $t = t_{\rm cluster}$) is simply called R, then we may write that

$$\frac{R_{\rm lock}}{R} = (\frac{t_{\rm cluster}}{t_{\rm lock}})^{\frac{1}{3}}. \quad (4)$$

Suppose, now, that a star is released to spin up at a time $t = t_{\rm lock}$ and conserves angular momentum between that time and the present. Then, since $\omega \propto R^2$ during times of angular momentum conservation, it is clear that

$$t_{\rm lock} = (\frac{\omega_{\rm lock}}{\omega})^{\frac{3}{2}} t_{\rm cluster} \quad (5)$$

must apply, where $\omega_{\rm lock}$ is the value of the stellar angular velocity just before the star is released from its disk and ω is simply the current angular velocity. We can use this expression to calculate $t_{\rm lock}$ for any star, given its measured ω and adopted values for $\omega_{\rm lock}$ and $t_{\rm cluster}$. Doing this for each star in the cluster allows us to reconstruct the history of disk unlocking in the ONC, subject of course to uncertainties in the adopted quanitites and the validity of the assumptions. Note that we have assumed that the age of a star is a constant in the ONC and equal to the age of the cluster. In other words, it is assumed that the age spread of stars within the cluster is small compared to $t_{\rm cluster}$. Whether these are reasonable assumptions will be discussed below, after we see what the model predicts.

6.1. Interpreting the rotation properties of the higher mass stars

If Eq. (5) is valid then we can determine, on the basis of its current rotation period, how long each star in the ONC was locked to its disk, assuming that $\omega_{\rm lock}$ is known. From the observed distribution of periods (assuming it is unbiased with respect to the presence or absence of disks or that we can correct for any bias – see below), we can then directly calculate the fraction of stars that were locked to their disks at any time in the past. Of course, it is not possible to know $\omega_{\rm lock}$ for any particular star but, since we still see a population of disk-locked stars, we can use their properties to constrain it in a statistical sense. Based on the slow rotators currently seen in the ONC, we adopt a normal distribution for $\omega_{\rm lock}$ with a mean of 0.8 rad/d (corresponding to a period of 7.85 days) and a width (1 σ) of 0.2 rad/d. On this basis we can construct a set of Monte Carlo models that demonstrate what disk-unlocking histories are consistent with today's observed distribution of ω. Before discussing the model results, however, it is necessary to deal quantitatively with the issue of a bias correction to the periodic sample.

As noted in Sect. 4 (see top panels of Fig. 13), the periodic star sample is non-representative of the full cluster in two respects. Namely, it is relatively depleted in stars with $\sigma < 0.01$ (i.e. non-variables) and also delpleted in stars with $\sigma > 0.1$ (i.e. likely CTTS). As the bottom panels of Fig. 13 show, the level of this incompleteness is not sufficient to cause any detectable differences in the infrared or v sin i characteristics of the periodic and non-periodic samples, so we could, with justification, ignore any bias correction. However, the clear and significant difference in σ distributions, coupled with the strong correlation between σ and infrared excess (Fig. 14) suggests that, perhaps, we should not do so, even though a large correction is clearly not warranted. We proceed to estimate a bias correction as follows. The relevant question for this discussion is how many stars with disks we have missed in the periodic sample (presumably because their irregular variations have made it impossible for us to determine their periods). Dividing the stars in the full sample (as displayed on Fig. 13) into three bins, by σ, yields the following numbers of stars in each bin: 75 ($\sigma < 0.01$), 495 ($0.01 < \sigma < 0.1$) and 197 ($\sigma > 0.1$). A similar division for stars in the periodic sample yields these numbers: 15, 234, and 48. Normalizing to the middle bin, where the periodic and non-periodic samples are essentially indistinguishable (see Fig. 13b), we find a deficiency of 20 stars in the low sigma bin and 45 stars in the higher sigma bin of the periodic star set. This yields a net deficiency of 25 stars likely to have disks which have been missed in the periodic star sample. This represents 8% of the total of 297 stars in that set. An 8% bias correction might be in order, therefore, but to be conservative we might adopt the more extreme value of 45/297 = 0.15. The models constructed in the rest of this paper include bias corrections of between 0 and 0.15, and their effect is simply to broaden the range of possible disk-unlocking histories which could be consistent with the current rotation data.

Our procedure is to select, for each star randomly, an $\omega_{\rm lock}$ from the initial distribution. If, by chance $\omega_{\rm lock} > \omega$ then the star is considered to be still locked to its disk, i.e. $t_{\rm lock} = t_{\rm cluster}$. Otherwise, $t_{\rm lock}$ is calculated from equation 5. This is done for the entire set of periodic variables and the disk-locking history (i.e. fraction of disk-locked stars as a function of time) formed. The process is repeated 100 times to understand the range of possible results which the Monte Carlo procedure can yield. A bias correction of 0.15 is then applied to the upper limit of these results, while no bias correction is applied to the lower limit. This effectively broadens our results to allow for the uncertainty in that correction factor. Figure 18 shows the results of applying this model to the observed rotation periods of stars with $M > 0.25\ M_{\odot}$. A cluster age of 1 My was adopted for this illustration. For comparison, we also show what would result from stochastic models in which disks become unlocked randomly in time using half lives ($t_{\frac{1}{2}}$) of 0.5, 0.7 and 1 My.

Two principal conclusions may be drawn from this exercise. First, based on stellar rotation alone (i.e. with no reference to infrared excess emission) we find that about 25–50% of the stars in the ONC should still be locked to their disks. This is somewhat smaller, but perhaps not significantly different, from the disk fractions estimated by infrared studies. Haisch et al. (2001) find a disk frequency in the Trapezium cluster (inner ONC) of 80% ± 5% based on JHKL photometry. This may not be directly comparable to our result because there is evidence that the Trapezium cluster is the youngest part of the ONC and that the disk frequency is higher there. Also, of course, we are measuring the number of stars *locked* to disks which may be less than the number of stars having disk emission. In our higher mass periodic sample, 60% of the stars have $\Delta(I-K) > 0.3$ mag. However, as Fig. 16 clearly shows, there are many stars also lying below the $\Delta(I-K) = -0.3$ mag level, which we take as evidence that the errors in calculating that quantity can be substantial. To increase the number of stars still locked to their disks would require increasing $\omega_{\rm lock}$ (i.e. lowering the assumed locking period) to well above what is reasonable. If the disk-locking hypothesis actually accounts for the bimodal period distribution and the correlation of rotation with infrared excess then no more than about one-half the stars in the ONC are currently locked to their disk, regardless of the infrared results.

A second result, which follows directly from the fraction of disk-locked stars is that the disk-locking time must be less than or comparable to the age of the cluster. A more careful comparison indicates that if we model the decay of disk-locking as a stochastic process, its half life must be about $0.5 - 1.0 t_{\rm cluster}$, or about 0.5–1.0 My for the nominal cluster age of 1 My. Again, we note that this is not necessarily the time for disk dissipation, which could be longer, but it is, nonetheless, a very short time! What ultimately breaks the disk lock is, of course, unknown, but one may speculate that it is unlikely to be the disappearance of the magnetic field, because rapidly rotating WTTS have substantial surface spots and are strong X-ray emitters. It is probably, therefore, the decline in accretion rate which must also mark the termination of the gas-disk phase. Hence, one may speculate that there will not be too great a time between the end of disk-locking and the disappearance of the accretion disk. Naturally, the planetesimal and (if applicable) planet disk can last indefinitely, assuming it has already formed and terrestrial planets can accumulate on much longer time scales. However,

giant planets must obviously form prior to the dissipation of the gas disk. Our constraint on disk-locking time, therefore, gives some additional impetus to the search for mechanisms that can form giant planets on timescales shorter than are required by standard models (see below).

The age of the cluster is, of course, somewhat uncertain and model dependent. Hillenbrand (H97) finds 0.8 My based on the D'Antona & Mazzitelli models, but it could, perhaps, be as old as 2 My if other models are applied (e.g. Palla & Stahler 1999). It is also possible, of course, that the age spread among the ONC stars is not small compared to the mean cluster age, as we have assumed. Palla & Stahler (2000), for example, propose that the observations favor an acceleration of star formation with time. However, Hartmann (2001) has argued persuasively against that view and Hartmann, Ballesteros-Paredes & Bergin (2001) have suggested that, in fact, rapid star formation is the norm in the galaxy. We conclude, therefore, that the time scale for disk-locking for the more massive stars cannot greatly exceed ~1 My in the ONC. This result has obvious implications for planet formation and drift, since it is shorter than the usual time scale quoted for the formation of massive planets. Boss (2001) has recently addressed the issue of giant planet formation and proposed that gravitational instability may be required instead of the commonly invoked core-accretion mechanism in the event that the disk disruption time scales are as short as ~1 My. The rotation evidence presented here, interpreted as an effect of disk-locking, provide additional support for the view that stars forming in clusters like the ONC would not generally have time to form giant planets by the core-accretion method. Of course, whether giant planets are to be found around ONC stars is currently unknown.

6.2. Interpreting the rotation properties of the lower mass stars

It is clear from Fig. 15 that the rotation properties of the lower mass stars in our sample differ in two respects from their higher mass counterparts: low mass stars appear to spin faster, on average, and they also do not reveal a bimodal period distribution. How can these differences be understood in terms of the physics of rotation and the evolution of the low mass star-disk systems? First, we note that the clear difference in period distribution is actually less of a difference in physically significant rotation properties than it may appear at first glance. A relevant point was already made in Paper I, where we showed that, in terms of specific angular momentum ($j = J/M$), there is actually only a small increase (~a factor of 2) as one moves from 1 to 0.1 $M_\odot$ stars. Also, while it is true that the lower mass stars spin at a much larger fraction of their critical velocity (typically 20% as opposed to 5% for the disk-locked solar-like stars) this comes about largely on account of the fact that $j_{\rm crit}$ declines significantly for the lower mass stars, owing to their smaller radii (see Fig. 3 of Paper I).

A key question is whether disk-locking is operative in the low mass stars. It may be seen on Fig. 16 that the trend apparent in the full sample, of declining infrared excess with increasing angular velocity, is actually present in *both* mass ranges. A Spearman test on both sub-samples confirms this, indicating nearly identical significance levels of less than 1 in $\sim 10^7$ that these correlations could arise from chance. It is clear that the more slowly rotating low mass stars do, indeed, tend to have evidence for circumstellar disks, supporting the view that disk-locking is involved in setting their rotation properties, just as it is for the higher mass stars. However, the level of infrared excess emission is clearly not as high as for the more massive stars. The mean value of $\Delta(I-K)$ for the 34 stars with $M < 0.25\ M_\odot$ and $\omega < 1$ is $\Delta(I-K) = 0.23 \pm 0.07$ (compared to 0.69 ± 0.07 for the higher mass stars), whereas the 80 stars in this mass range with $\omega > 2$ have a mean $\Delta(I-K)$ of 0.10 ± 0.06. Hence, while there is evidence of disks affecting rotation, there is also evidence that it is less important than for the more massive stars. We consider, in what follows, three possible explanations which alone, or in combination, could account for the trends seen, namely, disk-locking times may be shorter for low mass stars, disk-locking periods may be shorter, and/or lower mass stars may be generally older than higher mass ones.

It may be seen in Fig. 19 that the rotation distribution of the low mass stars, when displayed in terms of ω, rather than P, has some similarities to that of the higher mass stars. In particular, there is a distinct clump of slowly rotating stars and a tail of more rapid rotators. The main difference is that the two populations are more distinct in the case of the higher mass stars. The peak of the slowly rotating stars (i.e. those locked to disks or just recently released, in our interpretation) contains more stars and is at somewhat smaller ω and there are only half as many stars with ω in the range 1 to 3. This could mean that low mass stars do not stay locked to their disks for as long a period of time. This is certainly plausible since disk disruption in the ONC is currently proceeding at a rapid pace by evaporation in the intense ultraviolet radiation field of θ^1 Ori C and other members of the Trapezium. Evaporation times are expected to be shorter for low mass stars for two reasons: they probably have smaller disks to begin with and there is less of a gravitational well from which the heated disk gas must escape. To quantify the difference in locking times, we show in Fig. 20, that disk-locking times would need to be very short (~0.3 My) to account for the rotation distribution of the lower mass stars, if we assume they have the same locking period (7.85 days) as taken for the higher mass stars. This is one possible explanation for the observed differences and is supported by the generally lower values of infrared excess emission found for lower mass stars.

A second possibility is that the locking period is actually smaller for lower mass stars. In the analysis of Ostriker & Shu (1995), the stellar rotation period is equal to the Keplerian velocity at the locking radius, and may be written as (see also, Choi & Herbst 1996):

$$P_{\rm lock} \propto \frac{\mu^{\frac{6}{7}}}{\dot{M}^{\frac{3}{7}} M^{\frac{5}{7}}} \tag{6}$$

where μ is the magnetic moment, M is the stellar mass and $\dot{M}$ is the mass accretion rate. Clearly, the effect of $\dot{M}$ is least significant since it enters only as the 3/7th power. For the present analysis it should be sufficient to assume that $\dot{M} \propto M$.

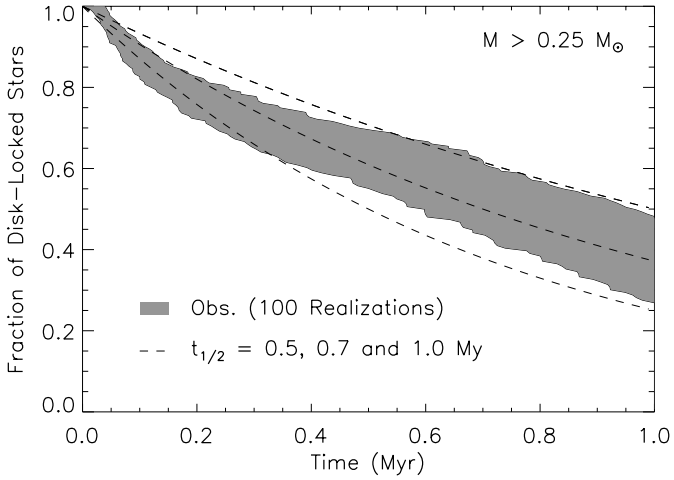

Fig. 18. The fraction of stars locked to their disks in the ONC as a function of time, as implied by the observed period distribution of the higher mass stars. For this example we chose locking periods ($\omega_{\rm lock}$) randomly from a normal distribution with a mean of 0.8 rad/d (period = 7.85 d) and a width of 0.2 rad/d. One hundred realizations are shown and all results fell within the bounds of the shaded region on the figure. A 15% bias correction, as discussed in the text, was included in calculating the upper limit on the observations. Also shown (dashed lines) are the predictions of a simple, stochastic model with disk half-lives of 0.5, 0.7 and 1.0 My, respectively from bottom to top. For this example, the age of the cluster ($t_{\rm cluster}$) was chosen to be 1 My. In general, we find that the data imply a disk-locking time of $0.7t_{\rm cluster}$, or 0.7 My in this case.

That leaves only the effect of μ to consider in evaluating the mass dependence of $P_{\rm lock}$. Since $\mu = B_*R^3$, we would need to know if and how the surface magnetic field strength, B_*, varies with the mass (effectively the photospheric temperature) to assess this definitively. Lacking such knowledge from either a theoretical or observational perspective, we assume here that the surface magnetic field strength is relatively independent of the temperature of the photosphere and, therefore, the mass of a PMS star. With the assumption of a constant B_*, it is clear that μ will decline precipitously with decreasing mass because, roughly, $R \propto M$ for such stars (e.g. D'Antona & Mazzitelli 1994; Palla & Stahler 1999). Using the expressions and approximations above, we find that $P_{\rm lock} \propto M^{\frac{10}{7}}$ should apply in the mass range 0.1–1 $M_\odot$. For the two samples discussed here, which differ in median mass by about a factor of 2, we would expect, therefore, a difference in the locking period of about a factor of 2.7, more than sufficient to explain the observations. In this case, the disk-locking times might be ∼0.7 My, similar to what was found for the higher mass stars.

A third possibility is that the lower mass stars are generally older than the higher mass stars. Since models of PMS stars are not sufficiently realistic to allow us to assign definitive ages to stars, it is not really possible to decide, on the basis of location on the HR diagram, what the age of a PMS star is. Here we note, that if the lower mass stars generally have ages of 2 My, compared to 1 My for the higher mass stars, then we can model their current rotation distribution well with exactly the same locking period (7.85 d) and half-life (0.7 My) as for the higher mass stars. The results of this model are shown in Fig. 21.

Our conclusion is that there are several potential effects that can lead to the differences between the higher and lower mass star rotations that have been observed in the ONC. At present, we cannot distinguish which, if any, is actually involved and at what level. It will be very interesting to see whether observations of rotation in different environments (say Taurus/Auriga or NGC 2264) yield the same differences in behavior with mass as we have found here. There could be implications for the formation of planets from this work. If it turns out that the rapid rotation arises from shorter disk locking times, which in turn implies quicker disruptions of the generally smaller mass disks, this could mean that there would not be enough time to form (at least massive) planets around low mass stars. Further implications of these results will be discussed in a forthcoming paper comparing the ONC rotation properties with what is found in the Taurus/Auriga association (Paper III) and in a new study of rotation in NGC 2264 (Lamm et al. 2002).

7. Summary and conclusions

The principal results of this investigation may be summarized as follows:

1) We have obtained light curves on an instrumental system close to Cousins I for more than 1500 PMS stars in the ONC. For stars between 12.5 and 16 mag, the data are sufficiently precise to allow us to characterize their variations and identify large numbers of periodic variables. For fainter stars, we can at least provide source identifications and a mean magnitude estimate. Comparison with previous studies suggests that a typical uncertainty in I magnitude of about 0.2 mag will apply to most stars in the ONC, presumably largely on account of variability. Some stars, of course, will vary much more than this. The general variability of ONC stars should be kept in mind when analyzing physical properties of the cluster such as the luminosity function and age spread.

2) Focusing on the subset of the data with highest precision (uncrowded stars with magnitudes between 12.5 and 16) we find that 297 of these 767 stars (39%) are periodic variables. Half of these 767 stars have variability ranges exceeding ∼0.2 mag, and 10% exceed ∼1 mag. Lower amplitude variables are more likely to be found periodic than are more active stars. 46% of the stars with $\sigma < 0.1$ mag were found to be periodic in this study, whereas only 24% of those with $\sigma > 0.1$ mag yielded periods. Variability correlates with infrared excess emission. These results are in agreement with the canonical view of PMS variability, namely that cool spots on WTTS are responsible for most or all of their variations, while hot spots on CTTS resulting from variable mass accretion from an inner disk contribute to their larger amplitudes, and more irregular behavior. The variability we see is, therefore, largely due to a combination of magnetically induced dark spots and a variable accretion process, with the latter becoming increasingly important for the higher amplitude variables.

3) This study resulted in the detection of 369 periodic variables, of which 111 had been found in previous studies. A comparison with previous results indicates that 99/111 periods agree to within the errors, while all but one of the remainder can be understood as an harmonic or beat period. The importance

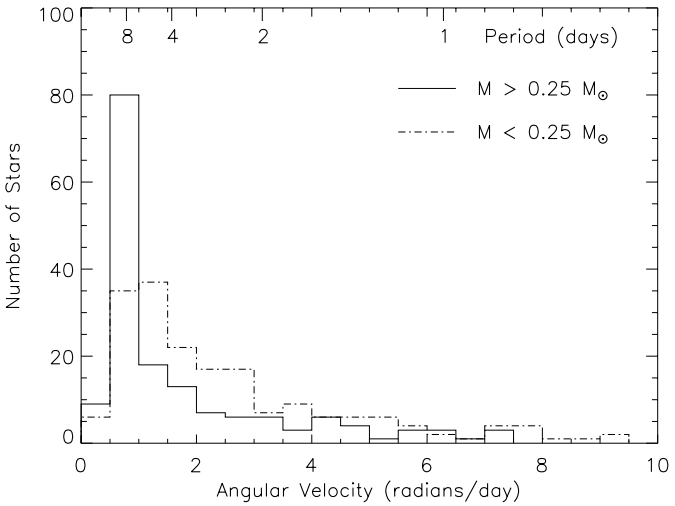

Fig. 19. Histograms showing the frequency distributions of angular velocity (ω) for stars in two different mass ranges. This is identical to Fig. 15 except in terms of ω rather than period. It emphasises the similarity in the rotation distributions of the stars in the two mass ranges, rather than their differences. However, the excess of rapid rotators among the low mass stars, particularly in the range ω = 1 to 3 is quite clear.

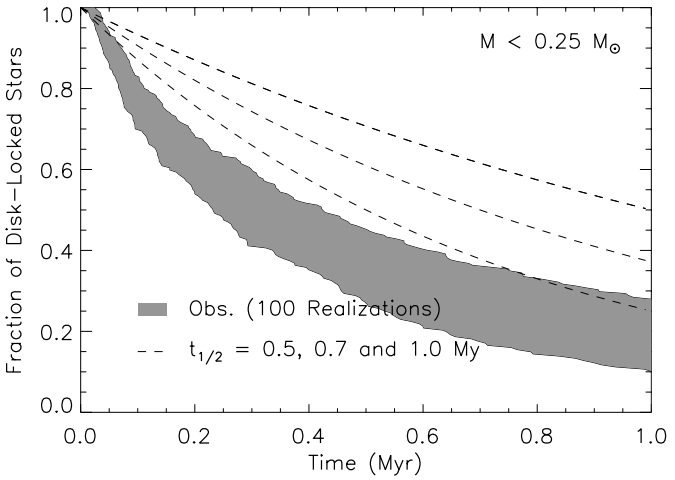

Fig. 20. Same as Fig. 18 but for the lower mass stars. For this example we chose locking periods ($\omega_{\rm lock}$) randomly from a normal distribution with a mean of 0.8 rad/d (period = 7.85 d) and a width of 0.2 rad/d. One hundred realizations are shown and all results fell within the bounds of the shaded region on the figure. Also shown (dashed lines) are the predictions of a simple, stochastic model with disk half-lives of 0.5, 0.7 and 1.0 My, respectively from bottom to top. For this example, the age of the cluster ($t_{\rm cluster}$) was chosen to be 1 My. Clearly, if the age and locking periods for the two mass samples are the same, then the more rapid rotation of the lower mass stars implies a smaller disk locking time, in this case about 0.3 My.

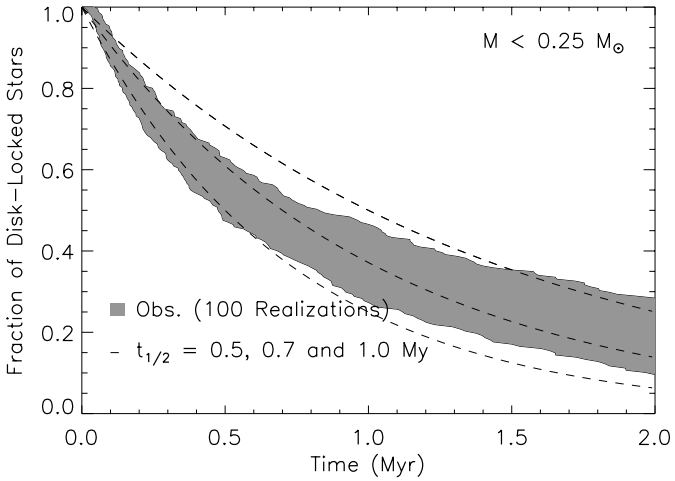

Fig. 21. Same as Fig. 20 but for an assumed cluster age of 2 My, instead of 1 My. If the lower mass stars are, in fact, on average twice as old as the higher mass stars then their rotation period distribution can be understood in those terms without recourse to smaller disk locking times or smaller initial disk locking periods. Nothing in our data or in H97 supports this particular model over the others; we discuss it only because it is a plausible explanation for our rotation data.

of both phenomena in period studies is discussed and illustrated in the text. About 15% of the periods found may be wrong, on account of these phenomena. Obviously, the effect will be most important in considering the extrema of the distributions.

4) It is confirmed that the period distribution for higher mass stars ($M > 0.25\ M_{\odot}$) is bimodal, while the period distribution for lower mass stars lacks the slowly rotating peak near 8 days and is dominated by rapidly rotating stars. The periodic stars are found to be only a slightly biased sample of the full cluster with respect to disk and rotation properties.

5) The long-suspected, but somewhat controversial, correlation between rotation and excess infrared emission, which is relevant to the disk-locking hypothesis, is finally confirmed at a very high significance level. There is no doubt now that more slowly rotating stars in the ONC have, on average, greater infrared excess emission than do their more rapidly rotating counterparts. Taking all masses together, the mean value of $\Delta(I-K)$ is 0.55 ± 0.05 for slow rotators ($\omega < 1$ rad d^{-1}) and 0.17 ± 0.05 for rapid rotators ($\omega > 2$ rad d^{-1}). As expected, there is a considerable amount of scatter in the relationship but a non-parametric statistical test shows that the probability that a correlation this good could be the result of chance is only $\sim 3 \times 10^{-11}$.

6) A simple, stochastic model for disk unlocking was explored in which stars conserve angular velocity until released from a disk-lock and then conserve angular momentum. If this is valid and if the initial period for the higher mass stars is near 8 days, then the time scale for these stars to be released from their disk locking in the ONC is slightly shorter than or comparable to the age of the cluster (corresponding to a half-life for disk unlocking of about 0.5–1 My). If disk unlocking occurs because of disk dissipation then there is not much time for giant planet formation among ONC stars.

7) We show that the angular velocity distribution of the low mass stars is similar, in many respects, to the higher mass stars. While the period distribution is not obviously bimodal, there is a broad clustering of slow rotators around a period of 4 days and a tail of rapid rotators. In both mass ranges there is a correlation of rotation with excess disk emission. We argue, therefore, that all ONC stars in the range 0.1−1 $M_{\odot}$ exhibit the effects of disk interactions on their rotation although it is more

apparent in the higher mass sample. We find that the differing rotation of the lower mass stars can be explained in several possible ways within the context of the disk-locking hypothesis. These include shorter disk-locking times and/or a shorter initial disk-locking period.

Acknowledgements. We thank the NASA-Origins program for their support of this work over a number of years. We thank Lynne Hillenbrand for many enlightening discussions of these issues over the years. We also thank John Carpenter, Karl Haisch and Luisa Rebull for providing data and other useful information and the referee, Lee Hartmann for his helpful and constructive report. WH would like to particularly express his gratitude to the staff of the Max Planck Institute for Astronomy in Heidelberg for their gracious hospitality during two extended visits and to Wesleyan University for its generous sabbatical policy.

References

Attridge, J. M., & Herbst, W. 1992, ApJ, 398, L61
Baraffe, I., Chabrier, G., Allard, F., & Hauschildt, P. H. 1999, A&A, 337, 403
Boss, A. P. 2001, ApJ, 563, 367
Bouvier, J., Bertout, C., Benz, W., & Mayor, M. 1986, A&A, 165, 110
Bouvier, J., Cabrit, S., Fernandex, M., Martin, E. L., & Matthews, J. M. 1993, A&A, 272, 176
Camenzind, M. 1990, Rev. Mod. Astron., 3, 234
Carpenter, J. M., & Hillenbrand, L. A. 2001, AJ, 121, 3160
Choi, P. I., & Herbst, W. 1996, AJ, 111, 283
D'Antona, F., & Mazzitelli, I. 1994, ApJS, 90, 467
Eaton, N. L., Herbst, W., & Hillenbrand, L. A. 1995, AJ, 110, 1735
Edwards, S., Strom, S. E., Hartigan, et al. 1993, AJ, 106, 372
Greene, T. P., & Lada, C. J. 1997, AJ, 114, 2157
Haisch, K. E., Lada, E. A., & Lada, C. J. 2001, ApJ, 553, L153
Hartmann, L. 2001, AJ, 121, 1030
Hartmann, L. 2002, ApJ, in press
Hartmann, L., Ballesteros-Paredes, J., & Bergin, E. A. 2001, ApJ, 562, 852
Hartmann, L. W., Soderblom, D. R., & Stauffer, J. R. 1986, AJ, 93, 907
Hayashi, M. 1965, PASJ, 17, 177
Herbst, W., Bailer-Jones, C. A. L., & Mundt, R. 2001, ApJ, 554, L197 (Paper I)
Herbst, W., Herbst, D. K., Grossman, E. J., & Weinstein, D. 1994, AJ, 108, 1906
Herbst, W., Maley, J. A., & Williams, E. C. 200, AJ, 120, 349
Herbst, W., Rhode, K. L., Hillenbrand, L. A., & Curran, G. 2000, AJ, 119, 261 (HRHC)
Hillenbrand, L. A. 1997, AJ, 113, 1733 (H97)
Hillenbrand, L. A., & Hartmann, L. W. 1998, ApJ, 113, 1733
Hillenbrand, L. A., Strom, S. E., Calvet, N., et al. 1998, AJ, 116, 1816 (H98)
Herbig, G. H., & Terndrup, D. M. 1986, ApJ, 492, 540
Horne, J. H., & Baliunas, S. L. 1986, ApJ, 302, 757
Jones, B. F., & Walker, M. F. 1988, AJ, 95, 1755
Krishnamurthi, A., Pinsonneault, M. H., Barnes, S., & Sofia, S. 1997, ApJ, 480, 303
Koñigl, A. 1991, ApJ, 370, L39
Lamm, M., Bailer-Jones, C. A. L., Mundt, R., & Herbst, W. 2002, in preparation
Lucas, P. W., & Roche, P. F. A. 2000, MNRAS, 314, 858
Mandel, G. N., & Herbst, W. 1991, ApJ, 383, L75
Mahdavi, A., & Kenyon, S. J. 1998, ApJ, 497, 342
O'Dell, C. R. 2001, ARA&A, 39, 990
Ostriker, E., & Shu, F. H. 1995, ApJ, 447, 813
Palla, F., & Stahler, S. W. 1999, ApJ, 525, 772
Palla, F., & Stahler, S. W. 2000, ApJ, 540, 255
Press, W. H., Teukolsky, S. A., Vetterling, W. T., & Flannery, B. P. 1992, Numerical Recipes (Cambridge U. Press, Cambridge)
Rebull, L. M. 2001, AJ, 121, 1676
Rhode, K. L., Herbst, W., & Mathieu, R. D. 2001, AJ, 122, 3258
Shu, F. H., Najita, J., Ostriker, E., et al. 1994, ApJ, 429, 781
Stassun, K. G., Mathieu, R. D., Mazeh, T., & Vrba, F. J. 1999, AJ, 117, 2941 (SMMV)